สมบัติทางการเสียดทานและการสึกหรอของคอมพอสิทจากพอลิเบนซอกซาซีนและ
ยางอะคริโลไนไทรล์-บิวทาไดอีนสำหรับการทำผ้าเบรกรถยนต์

นายจักรกฤช จันทรมหา

วิทยานิพนธ์นี้เป็นส่วนหนึ่งของการศึกษาตามหลักสูตรปริญญาวิศวกรรมศาสตรมหาบัณฑิต
สาขาวิชาวิศวกรรมเคมี ภาควิชาวิศวกรรมเคมี
คณะวิศวกรรมศาสตร์ จุฬาลงกรณ์มหาวิทยาลัย
ปีการศึกษา 2558
ลิขสิทธิ์ของจุฬาลงกรณ์มหาวิทยาลัย

FRICTION AND WEAR PROPERTIES OF POLYBENZOXAZINE/ACRYLONITRILE-
BUTADIENE RUBBER COMPOSITES FOR BRAKE PADS APPLICATION

Mr. Jakkrit Jantaramaha

A Thesis Submitted in Partial Fulfillment of the Requirements

for the Degree of Master of Engineering Program in Chemical Engineering

Department of Chemical Engineering

Faculty of Engineering

Chulalongkorn University

Academic Year 2015

Thesis Title	FRICTION AND WEAR PROPERTIES OF POLYBENZOXAZINE/ACRYLONITRILE-BUTADIENE RUBBER COMPOSITES FOR BRAKE PADS APPLICATION
By	Mr. Jakkrit Jantaramaha
Field of Study	Chemical Engineering
Thesis Advisor	Associate Professor Sarawut Rimdusit, Ph.D.

Accepted by the Faculty of Engineering, Chulalongkorn University in Partial Fulfillment of the Requirements for the Master's Degree

⋯⋯⋯⋯⋯⋯⋯⋯⋯⋯⋯⋯⋯⋯⋯⋯Dean of the Faculty of Engineering

(Associate Professor Supot Teachavorasinskun, D.Eng.)

THESIS COMMITTEE

⋯⋯⋯⋯⋯⋯⋯⋯⋯⋯⋯⋯⋯⋯⋯⋯Chairman

(Associate Professor Siriporn Damrongsakkul, Ph.D.)

⋯⋯⋯⋯⋯⋯⋯⋯⋯⋯⋯⋯⋯⋯⋯⋯Thesis Advisor

(Associate Professor Sarawut Rimdusit, Ph.D.)

⋯⋯⋯⋯⋯⋯⋯⋯⋯⋯⋯⋯⋯⋯⋯⋯Examiner

(Associate Professor Artiwan Shotipruk, Ph.D.)

⋯⋯⋯⋯⋯⋯⋯⋯⋯⋯⋯⋯⋯⋯⋯⋯External Examiner

(Associate Professor Siriwan Srisorrachatr, Ph.D.)

⋯⋯⋯⋯⋯⋯⋯⋯⋯⋯⋯⋯⋯⋯⋯⋯External Examiner

(Assistant Professor Chanchira Jubslip, D.Eng.)

จักรกฤช จันทรมหา : สมบัติทางการเสียดทานและการสึกหรอของคอมพอสิทจากพอลิเบนซอก
ซาซีนและยางอะคริโลไนไทรล์-บิวทาไดอีนสำหรับการทำผ้าเบรครถยนต์ (FRICTION AND
WEAR PROPERTIES OF POLYBENZOXAZINE/ACRYLONITRILE-BUTADIENE RUBBER
COMPOSITES FOR BRAKE PADS APPLICATION) อ.ที่ปรึกษาวิทยานิพนธ์หลัก: รศ. ดร.
ศราวุธ ริมดุสิต, 93 หน้า.

ในงานวิจัยนี้เป็นการพัฒนาวัสดุคอมพอสิทจากพอลิเบนซอกซาซีน (PBA-a) และอนุภาคยาง
อะคริโลไนไทรล์-บิวทาไดอีน (NBR) เป็นวัสดุเสียดทาน สำหรับประยุกต์ใช้ในการทำผ้าเบรครถยนต์ (อนุภาค
ยาง NBR ที่เราเลือกใช้ คือ อัลตราไฟน์-NBR (UNBR) และ ไมโคร-NBR (MNBR) เนื่องจากเป็นที่นิยมใน
อุตสาหกรรมผ้าเบรครถยนต์) โดยมีวัตถุประสงค์เพื่อศึกษาหาผลกระทบของปริมาณการเติมอนุภาคยางทั้ง 2
แบบที่มีต่อคุณสมบัติทางกายภาพ ทางกล ทางความร้อน ทางการเสียดทาน และการสึกหรอของวัสดุคอม
พอสิท จากผลการทดลองพบว่าค่าสมบัติต่างๆ ไม่ว่าจะเป็น ค่าสตอเรจมอดูลัส อุณหภูมิการเปลี่ยนสถานะ
คล้ายแก้ว สัมประสิทธิ์ความเสียดทาน และอัตราการสึกหรอ ของคอมพอสิท PBA-a/UNBR และ PBA-
a/MNBR ที่การเติมอนุภาคยางNBR แต่ละชนิด ปริมาณ 0, 2, 5, 10 และ 15 เปอร์เซ็นต์โดยน้ำหนัก มี
แนวโน้มเดียวกัน ซึ่งค่าสัมประสิทธิ์การเสียดทานของคอมพอสิท PBA-a/UNBR และ PBA-a/MNBR ทั้งหมด
ที่ทดสอบได้จากเครื่อง Pin-on-disc tribomer พบว่ามีค่าสูงขึ้นอย่างชัดเจนโดยจะสูงขึ้นเมื่อปริมาณอนุภาค
ยางในคอมพอสิทเพิ่มมากขึ้น จาก 0.50 ถึง 0.62 สำหรับ PBA-a/UNBR และ 0.50 ถึง 0.61 สำหรับ PBA-
a/MNBR นอกจากนั้นคอมพอสิทสามารถแสดงค่าอัตราการสึกหรอต่ำที่สุดที่ปริมาณการเติมอนุภาคยางแต่
ละชนิด 5 เปอร์เซ็นต์โดยน้ำหนัก เนื่องมาจากยางมีกระบวนการสูญเสียรูปเพื่อเพิ่มสภาพความเสียดทาน
และยังเป็นการป้องกันรอยแตกร้าวของคอมพอสิทอีกด้วย แต่ทว่าการเติมอนุภาคยางมากกว่า 10 เปอร์เซ็น
โดยน้ำหนักจะทำให้อนุภาคยางเกิดการเกาะกลุ่มกันเองทำให้เกิดการหลุดออกจากพื้นผิวของคอมพอสิทได้
ง่าย หลังจากนั้นนำคอมพอสิทที่เติมอนุภาคยาง UNBR 5 เปอร์เซ็นโดยน้ำหนักซึ่งเป็นสูตรที่ได้อัตราการสึก
หรอต่ำสุด ไปทดสอบสมบัติด้านการเสียดทานที่อุณหภูมิต่างๆ คือ 25, 100, 150, 200 และ 250 องศา
เซลเซียส พบว่าคอมพอสิทยังคงรักษาสภาพการเป็นวัสดุเสียดทานได้ดี ยิ่งไปกว่านั้นค่าสตอเรจมอดูลัสที่
อุณหภูมิห้องของคอมพอสิท PBA-a/UNBR และ PBA-a/MNBR ทั้งหมด ที่ตรวจวัดได้จากเครื่อง Dynamic
mechanical analyzer (DMA) มีค่าลดลงตามปริมาณการเติมอนุภาคยางที่เพิ่มมากขึ้น ส่วนอุณหภูมิการ
เปลี่ยนสถานะคล้ายแก้ว (T_g) ของคอมพอสิท PBA-a/UNBR และ PBA-a/MNBR พบว่า T_g ของคอมพอสิท
PBA-a/UNBR และ PBA-a/MNBR นั้นมีแนวโน้มเพิ่มขึ้นจาก 170 ถึง 188°C เมื่อเพิ่มปริมาณการเติม
อนุภาคยางแต่ละชนิด ลงในคอมพอสิท

ภาควิชา	วิศวกรรมเคมี	ลายมือชื่อนิสิต	....
สาขาวิชา	วิศวกรรมเคมี	ลายมือชื่อ อ.ที่ปรึกษาหลัก	....
ปีการศึกษา	2558		

5670136121 : MAJOR CHEMICAL ENGINEERING

KEYWORDS: FRICTION COMPOSITE / POLYBENZOXAZINE / ACRYLONITRILE BUTADIENE RUBBER / BRAKE PADS

JAKKRIT JANTARAMAHA: FRICTION AND WEAR PROPERTIES OF POLYBENZOXAZINE/ACRYLONITRILE-BUTADIENE RUBBER COMPOSITES FOR BRAKE PADS APPLICATION. ADVISOR: ASSOC. PROF. SARAWUT RIMDUSIT, Ph.D., 93 pp.

This research aims to develop acrylonitrile-butadiene rubber particles (NBR)-filled polybenzoxazine (PBA-a) composites as friction materials for brake pads application. The effect of types of NBR, i.e. ultrafine-NBR (UNBR) and micro-NBR (MNBR) on friction and wear, and thermomechanical properties of the PBA-a/NBR composites was investigated. From the results, the coefficient of friction of all PBA-a/UNBR and PBA-a/MNBR composites clearly increased with increasing rubber particle contents, i.e. 0.50-0.62 for the PBA-a/UNBR and 0.50-0.61 for the PBA-a/MNBR. In addiion, the lowest specific wear rate belonged the PBA-a filled with 5wt% of UNBR because the deformation of rubber particle plays a protective role against the wear damage of the composite. Whereas, the agglomeration of rubber particles was observed for the PBA-a filed with rubber particle over than 10wt%, resuting in an decrese in the specific wear rate due to easy detachment of NBR particles from the PBA-a matrix. Futhermore, the PBA-a/5wt% UNBR can maintain friction performance at temperature range of 25, 100, 150, 200 and 250°C. For the thermomechanical properties, the storage modulus at room temperature decreased with an increasing of rubber particle contents, while the PBA-a/UNBR and PBA-a/MNBR composites showed sinificantly high glass transition temperature found from the peak of loss modulus from dynamic mechanical analysis approximately 170-188°C.

Department:	Chemical Engineering	Student's Signature ....
Field of Study:	Chemical Engineering	Advisor's Signature ....
Academic Year:	2015	

ACKNOWLEDGEMENTS

CONTENTS

LIST OF FIGURES

LIST OF TABLES

CHAPTER I

INTRODUCTION

1.1 General Introduction

Automotive industry is one of the main industries of Thailand that generates economic value for the country. From Figure 1, Thailand's vehicle products are increased since 2006-2012. It accounts for 10% of gross domestic products originating from manufacturing and a source of employment more than 500,000 direct jobs of skill labors and above in 2012, not including value generated from related industries such as upstream industry, service industries such as financial, insurance and after sales service [1].
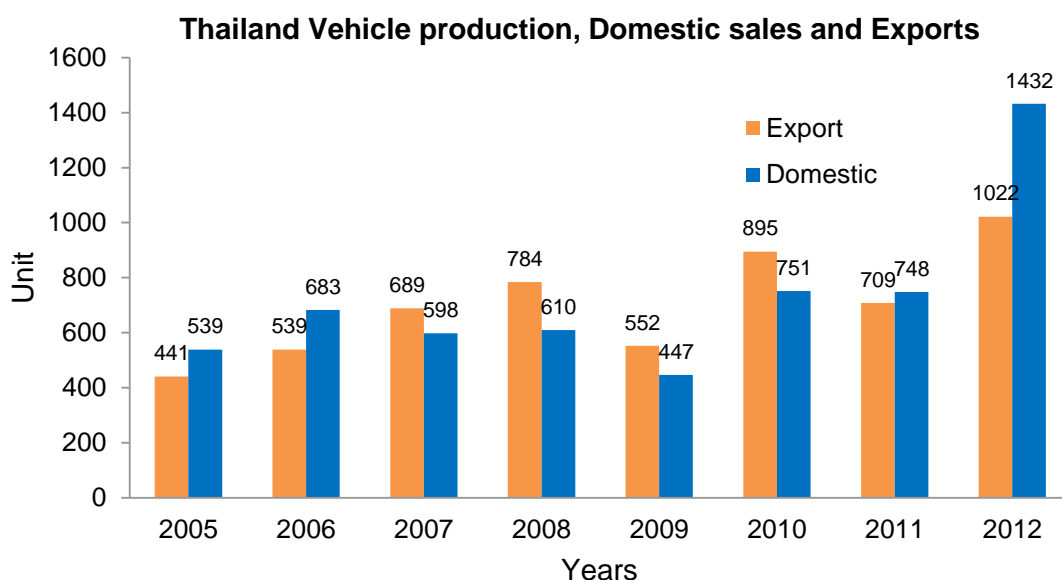
Figure 1.1 Thailand Vehicle production, Domestic sales and Exports (Source: The Federation of Thai Industries/MBKET) [1].

Furthermore, Thailand is a leading regional and global automotive manufacturer, ranks the first among ASEAN countries and 15th in the world in 2012 and also a major regional production base for automotive parts [1, 2]. Brake pad is one of the most important safety parts in a vehicle which has major function is to stop or to reduce speed of a vehicle [2, 3]. Generally, friction materials used as brake pads comprise four classes of ingredients i.e. binders, fillers, reinforcing fibers and frictional additives that included abrasive and lubricant [4-6]. In this work, we focus on the effects of acrylonitrile-butadiene rubber on properties of a novel type of binder i.e. polybenzoxazine to be used as friction materials. Major properties such as mechanical, tribological and thermal properties are to be investigated.

Binders are important ingredient for maintaining structural integrity of the brake pads under mechanical and thermal stresses. In principle, the proportion of binder in the pads material is largely dictated by the required performance of the pads [7]. Conventional brake pads use phenolic resin as binder in friction materials because of high thermal stability, chemical resistant and flame retardant. However, most phenolic resins still have some shortcomings such as a need of catalysts in synthesis step, release of by-product during processing and its brittleness [8]. Furthermore, Kurihara et al. had suggested the use of polybenzoxazine as binder for friction materials as disclosed in US 8,227,390 B2 [8]. They explained the case of a friction material using phenolic resin (PF) to show a molding failure i.e. cracks. The cracks generated during a polymerization step because of a gas by-product formed. Moreover, there is a concern

about environmental pollution by ammonia as a main component of the gas. To overcome the inherent problems [9] from using phenolic binder, the new types of phenolic resins called benzoxazine resins (BA-a) have been proposed as a replacement for traditional phenolic resins, A benzoxazine resin that no gas generates in polymerization step and can improved friction material excellent in heat resistance and strength is used with an attempt to substitute for phenolic resin or epoxy resin.

Benzoxazine resins (BA-a) are a novel kind of thermosetting phenolic resins that can be synthesized from amine, formaldehyde and phenol. The resins can undergo ring-opening polymerization without the use of catalysts or curing agents and do not produce by-products upon curing [10]. Polybenzoxazine has outstanding properties such as low melt viscosity before curing, high glass transition temperature (T_g) and high thermal stability as well as excellent mechanical properties. Furthermore, polybenzoxazine possess a relatively good dimensional stability after curing with low water absorption characteristics [10-14] thus makes these polymers highly useful in vast applications such as highly filled composites.
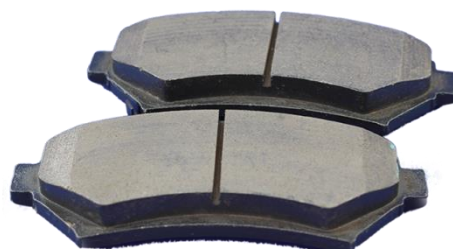
Figure 1.2 Commercial disc brake pads [15]

Fillers including substances such as rubber particles, barite ($BaSO_4$), calcite ($CaCO_3$), and mica (a silicate mineral group) are frequently incorporated in the brake pads materials in order to reduce manufacturing costs, improve some properties and manufacturability [4]. In particular, rubber particle fillers can be added to suppress brake noise, improve toughness and impact strength of friction materials. Incorporating rubber components into resin-based materials is a conventional method to improve flexibility and damping properties of the resulting polymer products [16, 17]. The rubber components are usually integrated in the resin matrix by physical or chemical methods. Bijwe et al. [5, 6, 18] investigated acrylonitrile-butadiene rubber (NBR) chemically modified PF and found that the NBR modification resulted in an improvement in recovery performance of composites. Liu et al. [19] reported two kinds of PF, chemically modified by grafting to rubber particles, that were prepared and investigated as a matrix for organic brake pads and they found the friction material based on the modified PF with more internal friction generating units possessed much higher impact and compression strengths, greater toughness, and better braking stability.

Reinforcing fibers had provided mechanical strength of friction material, various metals, carbon, glass, and Kevlar (the trademark name of a lightweight synthetic fiber of exceptionally high strength and heat resistance) are commonly used, and to a lesser extent, mineral and ceramic fibers [20, 21]. Recent researched by Eriksson had reported

that friction material wear will increased with a decreasing amount of reinforcing fiber [22].

Frictional additives are components added to friction materials in order to modify the coefficient of friction (COF) as well as the wear rates [21, 22]. They are divided into two main categories i.e. lubricants and abrasives. Lubricants assist in stabilizing frictional properties, particularly at high braking temperatures. Common examples include graphite and various metal sulphides such as antimony trisulphide (Sb_2S_3) [23]. Abrasives serve to increase friction, maintain cleanliness between contact surfaces and limit the build-up of transfer films. A variety of substances have been employed as abrasive additives including aluminium oxide, iron oxides, quartz (silicon oxide), and zircon (zirconium silicate).

The use of nano-particles in polymers for tribology performance enhancement started around mid-1990s [24] and this area has become quite promising for the future as newer nanomaterials are being economically and routinely fabricated. In most of the cases, a polymer nanocomposite relies for its better mechanical properties on the extremely high interface area between the filler (nano-particles or nano-fibers) and the matrix (a polymer) [19]. High interface leads to a better bonding between the two phases and hence better strength and toughness properties over unfilled polymer or traditional polymer composites. For all polymer/nano-particle systems [25], there will be an optimum amount of the nanoparticles beyond which there will be a reduction in the toughness as the stiffness and strength increase.

This research aims to study and compare behaviors of micro- and ultrafine-NBR fillers in a novel binder based on PBA-a matrix and will evaluate some important parameters for an application as friction materials. Those essential properties include glass transition temperature, COF, and wear rate to determine friction material performance of the obtained PBA-a/NBR composite systems

1.2 Objectives

1. To develop ultrafine-NBR modified polybenzoxazine composites for friction materials.

2. To examine interfacial bonding between NBR filler and the polybenzoxazine matrix.

3. To evaluate effects of the ultrafine-rubber contents on thermal, mechanical, friction and wear properties of the obtained polybenzoxazine composites.

4. To compare thermal, mechanical, friction and wear properties of micro-NBR and ultrafine-NBR powder on the resulting polybenzoxazine composites.

1.3 Scope of the study

1. Synthesis of bisphenol-A-aniline based benzoxazine resin (BA-a).

2. Preparation of the benzoxazine resin filled with ultrafine-NBR as well as micro-NBR modifier at various weight percentages in a range of 0 to 15%.

3. Study on possible intermolecular interactions of the benzoxazine resin filled

with those NBR powders by Fourier transform infrared spectroscope (FTIR).

4. Investigation of thermal, mechanical and tribological properties of the benzoxazine resins filled with ultrafine-NBR and micro-NBR by:

    a. Differential scanning calorimeter (DSC).

    b. Dynamic mechanical analyzer (DMA).

    c. Thermal gravimetric analyzer (TGA).

    d. Coefficient of friction and wear resistance

5. Investigation of the interfacial bonding between NBR filler and polybenzoxazine by scanning electron microscopy (SEM).

6. Development of the PBA-a/NBR to applied brake pads application.

1.4 Procedure of the study

1. Reviewing related literature.

2. Preparation of chemicals and equipment to be used in this research.

3. Synthesis of benzoxazine resins (BA-a) by solventless technique.

4. Preparation of composites between benzoxazine resins (BA-a) and ultrafine powdered rubber (ultrafine-NBR) as well as micro-NBR at various mass ratios.

5. Determination of thermal, mechanical and some tribological properties of PBA-a/NBR composite as follows:

    a. Coefficient of friction

    b. Wear rate

     c.   Degradation temperature at 5wt% loss ($T_{d,5}$)

     d.   Glass transition temperature (T_g)

     e.   Storage modulus

6.   Analysis of the experimental results.

7.   Preparation of the final report.

CHAPTER II
THEORY

2.1 Type of Friction Material

The materials used in a brake system unit have a great effect on its stopping ability. More force is needed to move some materials over a surface than others, even when applied pressure, contact area, and finish are the same. The friction characteristics of a brake material make up its coefficient of friction. If the coefficient of friction is too high, the brakes will work too well and cause the wheels to lock up. If the coefficient of friction is too low, the brake pedal would require excessive force to stop the vehicles [26].

Brakes are now manufactured from a variety of different materials that may be:

- non-asbestos organic

- low metallic

- semi-metallic

- ceramic etc.

2.2 Coefficient of friction (COF) or Friction Coefficient

From Figure. 2.1 friction coefficient or coefficient of friction (COF) mean friction is always present between two materials that slide against each other. The coefficient of friction is the amount of friction that can be produced as two materials slide across

each other. In other word coefficient of friction that simple to find ratio of friction force to normal force. The coefficient of friction is determined by a simple calculation. In the example shown in Figure 2.2, the coefficient of friction is calculated by measuring the force required to slide a block over a surface and then dividing it by the weight of the block [27].
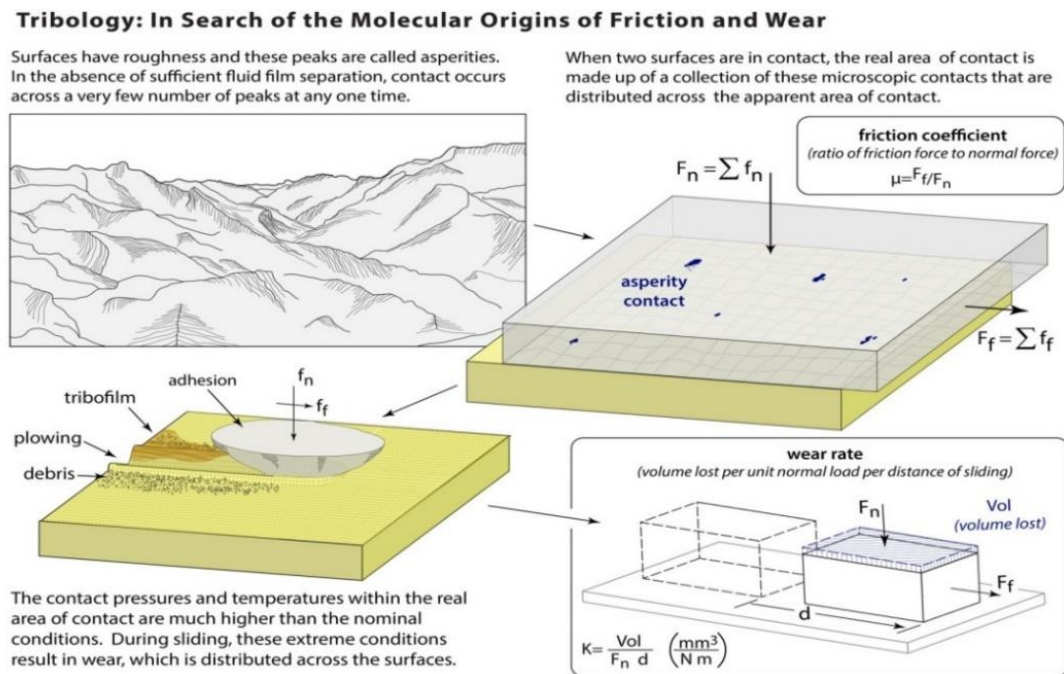
Figure 2.1 Tribology theory [28]

JIS (Japanese industrial standard) had classified COF of brake pads, based on data obtained from tests conducted in accordance with JIS D 4411 and Thailand industrial standard shown in Table 2.1.

Table 2.1 Classification

Classification	Use
Class 1	Used only for parking brake those use for center brake, drum brake of drum in disc brake, etc.
Class 2	Drum brake use for light load
Class 3	Drum brake use for heavy load
Class 4	Used for disc brake

Table 2.2 Class 1

Item	Test temperature (^{o}C)		
	100	150	200
Coefficient of friction	0.30 to 0.70	0.25 to 0.70	0.20 to 0.70
Wear rate (10^{-4}mm^{3}/Nm)	1.0 or less	2.0 or less	3.0 or less

Table 2.3 Class 2

Item	Test temperature (^{o}C)			
	100	150	200	250
Coefficient of friction	0.25 to 0.65	0.25 to 0.65	0.20 to 0.70	0.15 to 0.70
Wear rate (10^{-4}mm^{3}/Nm)	0.5 or less	0.7 or less	1.0 or less	2.0 or less

Table 2.4 Class 3

Item	Test temperature (°C)				
	100	150	200	250	300
Coefficient of friction	0.25 to 0.65	0.25 to 0.70	0.25 to 0.70	0.20 to 0.70	0.15 to 0.70
Wear rate $(10^{-4}mm^3/Nm)$	0.5 or less	0.7 or less	1.0 or less	1.5 or less	3.0 or less

Table 2.5 Class 4

Item	Test temperature (°C)					
	100	150	200	250	300	350
Coefficient of friction	0.25 to 0.65	0.25 to 0.70	0.25 to 0.70	0.25 to 0.70	0.25 to 0.70	0.20 to 0.70
Wear rate $(10^{-4}mm^3/Nm)$	0.5 or less	0.7 or less	1.0 or less	1.5 or less	2.5 or less	3.5 or less
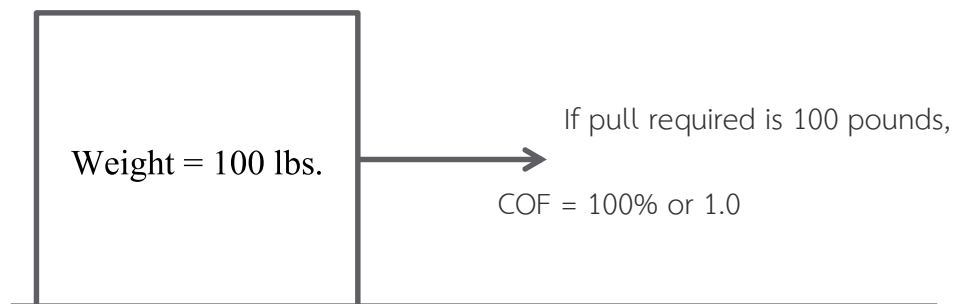
Figure 2.2 Example to calculate the coefficient of friction

2.3 Wear Rate

Wear rate is strongly influenced by the operating conditions. Specifically, normal loads and sliding speeds play a pivotal role in determining wear rate [29]. Furthermore, tribo-chemical reaction is also important in order to understand the wear behavior. Different oxide layers are developed during the sliding motion [30]. The layers are originated from complex interaction among surface, lubricants, and environmental molecules. In general, a single plot, namely wear map. Demonstrating wear rate under different loading condition is used for operation.

The specific wear rate (W_s) is calculated as follows [31, 32]

$$W_s = [(W_1 - W_2) \times \frac{10^3}{\rho}]/Pvt \qquad (2.1)$$

Where

W_s (mm^3/N·m)　　is the specific wear rate

W_1 (g)　　　　　　is the weight before test

W_2 (g)　　　　　　is the weight after test

ρ (g/cm3)　　　　is the density of sample

P (N)　　　　　　is the applied normal load

v (m/s)　　　　　is the relative sliding velocity

t (s)　　　　　　is the experimental time

2.4 Factors Affecting Braking

2.4.1 Static and Kinetic Friction

The two basic types of friction are stationary or static friction and kinetic friction, sometimes called sliding or dynamic friction. The static friction is a holding action that keeps a fixed object in place, while kinetic friction reduces a moving object by converting momentum to energy. The static friction is always higher than kinetic friction. The most apparent use of static friction is the parking brake [33]. When the parking brake is applied, static friction between the applied brake components resists movement. To move the vehicle, static friction must be eliminated by releasing the brakes. Since the vehicle has no movement, there is no momentum to overcome, and no heat is generated [34].

2.4.2 Friction Material Temperature

The temperature of the friction materials has a large effect on the amount of friction developed. As the friction material higher temperature, the ability to stop the vehicle was reduced. Not only must friction materials be designed to operate under significantly varying temperatures, they have roughly the same coefficient of friction, both lower and higher temperatures. Too much variation means the brake pedal feel and required pressure would change drastically as the brakes become heated [34, 35].

2.4.3 Apply Pressure

The more pressure applied to the brake friction members, the more they resist movement, and the more friction is developed. More friction means more braking

action. Pressure is created by a combination of mechanical leverage and hydraulic

pressure, plus the action of the power assist unit [34, 36].
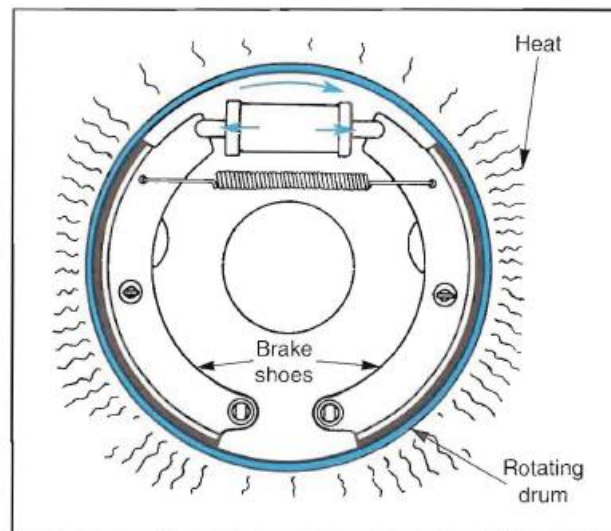
Figure 2.3 Static friction (not moving) with the parking brake shoes expanded into contact with the inside hub (drum), the rotor is prevented from turning. B-Exploded view of the various brake components [34].

2.4.4 Friction Material Contact Area

While a small braking surface could generate as much friction as a larger

surface by being applied harder, it would rapidly overheat and become use fewer.

Brake friction members must be large enough to absorb and spread the frictional heat

out. For this reason the larger the vehicle, the larger the brake friction components

[34].

2.4.5 Tire and Road Conditions

If the tires do not grip the road properly, the brake system will not work. Traction between the tires and the road must be maintained for proper stopping. If the brake system works so well that the tire stops rotating, it is said to be skidding [37, 38]. When the road is wet or icy, the tire is skidding on a layer of water or ice. On dry pavement, a skidding tire causes so much frictional heat that the tire rubber melts. The tire then skids on a layer of liquid rubber [34].

2.4.6 Weight Transfer

When a vehicle is at rest, most of the vehicle weight is over the front wheels, since the engine and transmission are at the front of the vehicle. As much as 60% of the total weight of a rear-wheel drive vehicle is supplied by the front wheels [34, 39].

2.5 Non-Asbestos Organic (NAO) Friction Material

Organic formulations often contain polymers such as Kevlar, resins, and sometimes asbestos fibers. Organic brake pads may also contain copper. In the past, asbestos was used extensively in organic formulations before it was discovered that breathing dust containing asbestos fibers can cause serious bodily harm [40]. Today, although use of asbestos is still legal, manufacturers are generally moving towards non-asbestos organic formulations for safety reasons. The four main components of a brake pad, namely the reinforcing fibers, binders, fillers and frictional additives, are

discussed below. It is important to note that certain substances perform multiple functions and may be placed in more than one classification [4, 22].

- Reinforcing fibers: provide mechanical strength. Various metals, carbon, glass, and Kevlar (the trademark name of a lightweight synthetic fiber of exceptionally high strength and heat resistance) are commonly used, and to a lesser extent, mineral and ceramic fibers. Fibers comprise between 6 and 35% of brake pad mass [20, 23].

- Frictional additive: Abrasives, serve to increase friction, maintain cleanliness between contact surfaces and limit the build-up of transfer films, and typically account for up to 10% of the brake pad materials. A variety of substances have been employed, including aluminum oxide, iron oxides, quartz (silicon oxide), and zircon (zirconium silicate) [23]. Lubricants, make up 5–29% of the brake pads, and assist in stabilizing frictional properties, particularly at high braking temperatures. Common examples include graphite and various metal sulphides e.g. antimony trisulphide (Sb_2S_3) [22].

- Fillers: substances such as barite ($BaSO_4$), calcite ($CaCO_3$), and mica (a silicate mineral group) that are incorporated to reduce manufacturing costs and improve manufacturability. The abundance of fillers varies from 15 to 70% [16, 17].

- Binders: important for maintain structural integrity of the brake pads under mechanical and thermal stresses. The proportion of binder in material is largely dictated by the required performance of the brake pads, but account for 20–40%. Phenolic resins are widely used as binders [7].

2.6 Polybenzoxazine

Polybenzoxazine is a novel type of phenolic resin with interesting properties that are based on the ring opening polymerization of benzoxazine precursors. As a novel class of phenolic resin, it has been developed and studied to overcome several short comings of conventional novolac and resole-type phenolic resin. Polybenzoxazine resins are expected to replace traditional phenolic, polyesters, vinyl esters, epoxies, cyanate esters and polyimides in many respects [41]. The mechanical and physical properties can be tailored to various needs. The material can be synthesized using the patented solventless technology to yield a relatively clean precursor without the need of solvent elimination or monomer purification [11, 41-43].

Polybenzoxazine can be synthesized from inexpensive raw materials and can be cured without the use of strong acid or base catalyst. The resins can undergo ring-opening polymerization without catalysts or curing agents and do not release

by-products upon curing. The polybenzoxazine has excellent properties, commonly found in traditional phenolic resins such as high thermal stability, flame retardant, dimensional stability, low melt viscosity, near-zero shrinkage upon polymerization, low water absorption, high mechanical integrity, glass transition temperatures much higher than cure temperature, fast mechanical property build-up as a function of degree of polymerization, high modulus and high char-yield thus makes these polymers highly useful in vast applications such as highly filled composites [11, 14, 41, 42, 44].

Benzoxazine resin based on bisphenol-A and aniline is synthesized according to the following reaction scheme as shown in Figure 2.4 [45].

Benzoxazine monomer
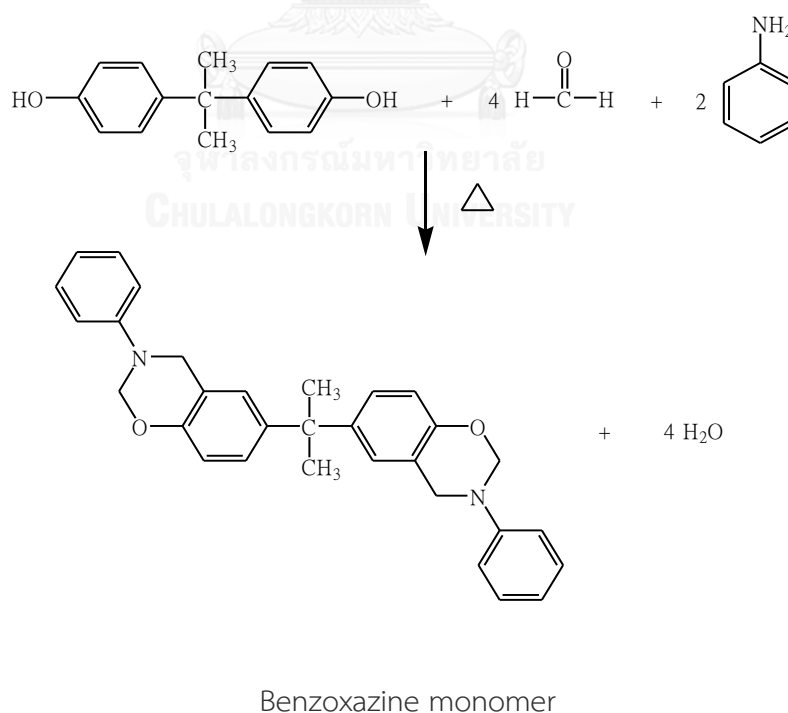
Figure 2.4 Synthesis of bifunctional benzoxazine monomer [44, 45].

The properties of polybenzoxazines compared with those of the state of art matrices were depicted in Table 2.2. Polybenzoxazines present the highest tensile properties. Their results from dynamic mechanical analysis reveal that these candidate resins for composite applications possess high moduli and glass transition temperatures, at low cross-link densities. Long-term immersion studies indicate that these materials have a low rate of water absorption and low saturation content. Impact, tensile, and flexural properties are also good [40, 44, 45].

Table 2.6 Comparative properties of various resins [45].

Property	Epoxy	Phenolic	Cyanate Ester	PBA-a
Density (g/cm^3)	1.2 - 1.25	1.21 - 1.32	1.1 - 1.35	1.19
Max use temperature (^{o}C)	180	200	150-200	130 - 280
Flexural strength (MPa)	90 – 120	24 – 45	70 – 130	127 - 148
Tensile modulus (GPa)	3.1 - 3.8	0.3-0.5	3.1 - 3.4	3.8 - 4.5
Elongation (%)	3 - 4.3	0.3	0.2-0.4	2.3 - 2.9
Dielectric constant (1 MHz)	3.8 – 4.5	04/10	2.7 - 3.0	3 - 3.5
Cure temperature (^{o}C)	RT – 180	150 – 190	180 – 250	160 - 220
Cure shrinkage (%)	> 3	0.002	3	~ 0

TGA onset (°C)	260 – 340	300 – 360	400 – 420	380 – 400
T_g (°C)	150 – 220	170	250 – 270	170 - 340

*Phenolic resins, Epoxy resins, Cyanate ester resins, Benzoxazine resins, Thermogrvimetric analysis (TGA), Fracture energy (GIC), Fracture toughness plain-strain stress intensity factor

2.7 Acrylonitrile-Butadiene Rubber

Acrylonitrile-butadiene rubber (NBR), also called nitrile-butadiene rubber, an oil-resistant synthetic rubber made from a copolymer of acrylonitrile and butadiene. Applications of NBR are in fuel hoses, gaskets, rollers, and other products in which oil resistance is required. The chemical structure of NBR [46] as seen in Figure 2.5.
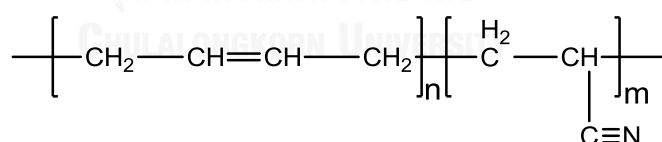
Figure 2.5 Acrylonitrile-butadiene rubber chemical structures.

In the production of NBR, acrylonitrile ($CH_2=CHCN$) and butadiene ($CH_2=CH-CH=CH2$) are emulsified in water and then polymerized [18, 47] (their single-unit molecules linked into large, multiple-unit molecules) through the action of free-radical initiators. On a cost basis, nitrile, or NBR, rubber is the least expensive of the oil resistant

elastomers. As a result, nitrile rubber is one of the most widely used rubber materials due to its combination of low cost, resistance to many chemicals, and good physical properties. The acrylonitrile content of this highly polar elastomer provides excellent oil and gas permeation resistance which increases as the level of ACN increases [46]. Unfortunately, an increase in the acrylonitrile content compromises low temperature flexibility, increases compound hardness and glass transition temperature. Typical ACN content ranges from 18% to 50%. Nitrile should not be exposed to direct sunlight or moderate to high levels of atmospheric ozone, as rapid deterioration will result. However, NBR will accept many antidegradants, most notably PVC, which offer some degree of improvement of these properties. Nitriles are usually sulfur cured, but peroxide curing is also possible, resulting in improved compression set.

Nitrile rubber, like styrene-butadiene rubber and other synthetic elastomers (elastic polymers), was a product of research that took place during and between the two world wars. A group of acrylonitrile-butadiene copolymers, given the name Buna N, was patented in 1934 by German chemists Erich Konrad and Eduard Tschunkur [48], working for IG Farben. Buna N was produced in the United States during World War II as GR-N (Government Rubber-Nitrile), and subsequently the group of acrylonitrile-butadiene elastomers became known as nitrile rubber.

CHAPTER III

LITERATURE REVIEWS

Ning and Ishida [42] synthesized bifunctional benzoxazine. The polyfunctional benzoxazine (BA-a) was found to exhibit excellent mechanical and thermal properties with good capability for processing and composite manufacturing, i.e., tensile modulus of 3.2 GPa, and tensile strength of 58 MPa. Furthermore, they reported the BA-a more flexibility than conventional phenolic resins in terms of molecular design, no by-products during polymerization step and no solvent needed in the resin synthesized.

Ishida and Allen [49] studied the properties of polybenzoxazine thermosetting resins based on the ring-opening polymerization of benzoxazine precursors (BA-a, BA-m). They synthesized from inexpensive raw materials and undergo polymerization by a ring opening reaction and no released by-product in curing step. Benzoxazine resins cure without catalysts generally required by traditional phenolic resins. Dynamic mechanical analysis found that high moduli and high glass transition temperature with low crosslink densities, i.e., flexural modulus ca. 3.8 to 4.5 GPa, flexural strength ca. 103 to 126 MPa, and T_g ca. 170 to 180°C. Polybenzoxazines have significantly higher tensile moduli than both phenolics and epoxies just maintain adequate tensile strength and impact resistance. In addition, low water absorption and

good dielectric properties allow these materials to perform well in electronic applications.

Lu et al. [50] investigated effect of components on friction performance of polybenzoxazine filled with soft (graphite, MoS_2 and Twaron/aramid pulp) and hard (aluminium, oxide and steel wool) additives for automotive friction materials. The authors reported that the addition of each aluminium oxide or steel wool to polybenzoxazine initially causes an increase in friction coefficient (μ), i.e., 0.78 for aluminium oxide and 0.73 for steel wool while the addition of graphite reduced the initial friction coefficient of polybenzoxazine from 0.5 to a value of 0.26 as shown in Figure. 3.1, the average friction coefficient of Twaron filled polybenzoxazine is around 0.35 as shown in Figure. 3.2. In addition, the wear-composition relationships of the polybenzoxazine filled with soft and hard additives as seen in Figure. 3.3 and Figure 3.4 respectively. From the figure, the lowest wear and minimum volume of polybenzoxazine are 22.26% and 0.236, respectively, for polybenzoxazine filled with aluminium oxide and 11.53% and 0.382, respectively, for polybenzoxazine filled with steel wool. The minimum volume loss due to wear of polybenzoxazine binder reflects the good adhesion between the additives and the resin binder. In the case of polybenzoxazine filled with soft additive, the lowest wear was found to be 5.38% for polybenzoxazine filled with Twaron. However, in general, the Twaron or aramid pulp use as reinforcing fiber in friction materials usually enhanced the mechanical strength and reduce the thermal conductivity of resulting the friction materials as well.
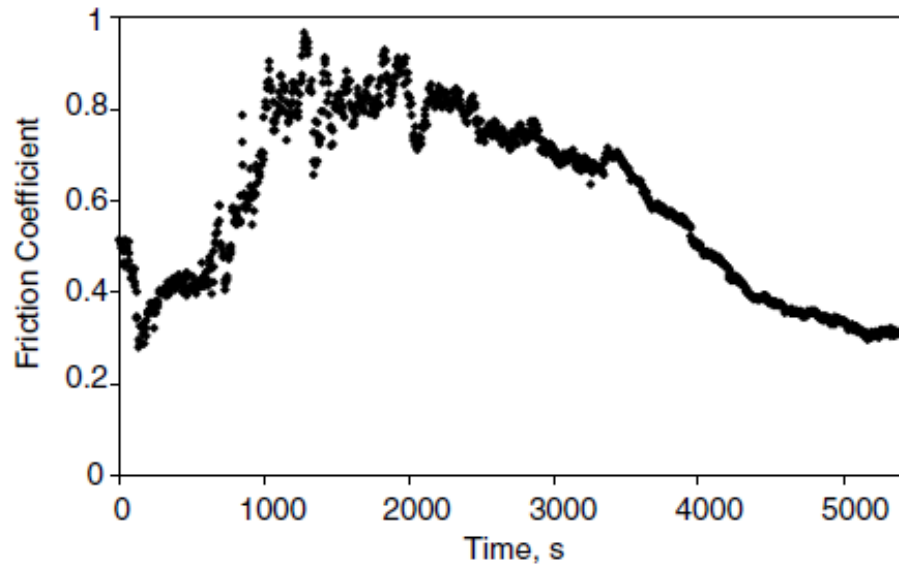
Figure 3.1 Friction Assessment and Screening Test (FAST) under a constant friction force 17.4 N, run at the disc rotation speed of 6.96 m/s for 90 min of polybenzoxazine [50].
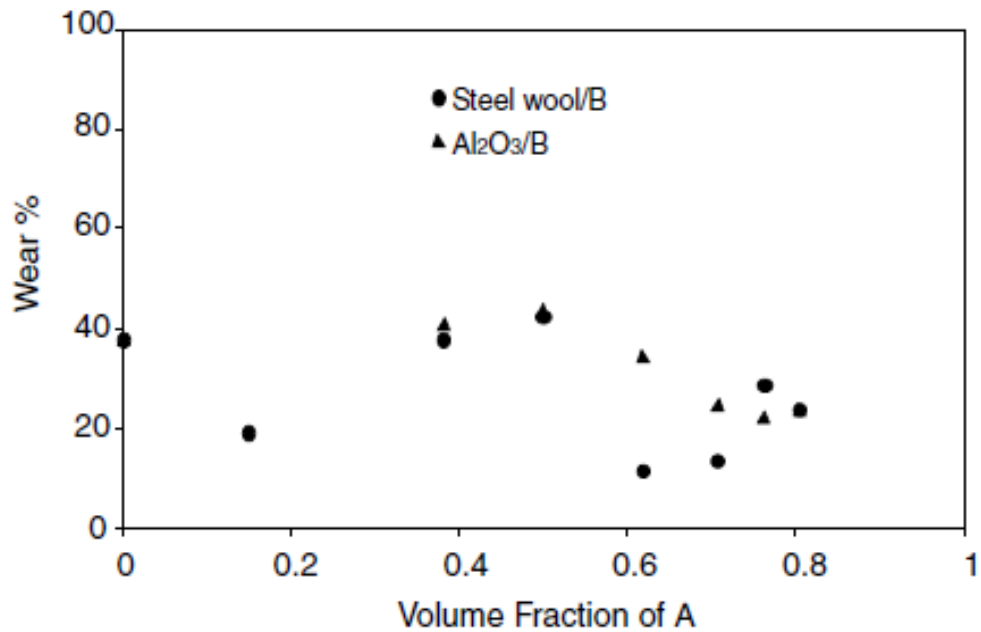
Figure 3.2 FAST curve under a constant friction force 17.4 N, run at the disc rotation speed of 6.96 m/s for 90 min of Twaron filled polybenzoxazine [50].
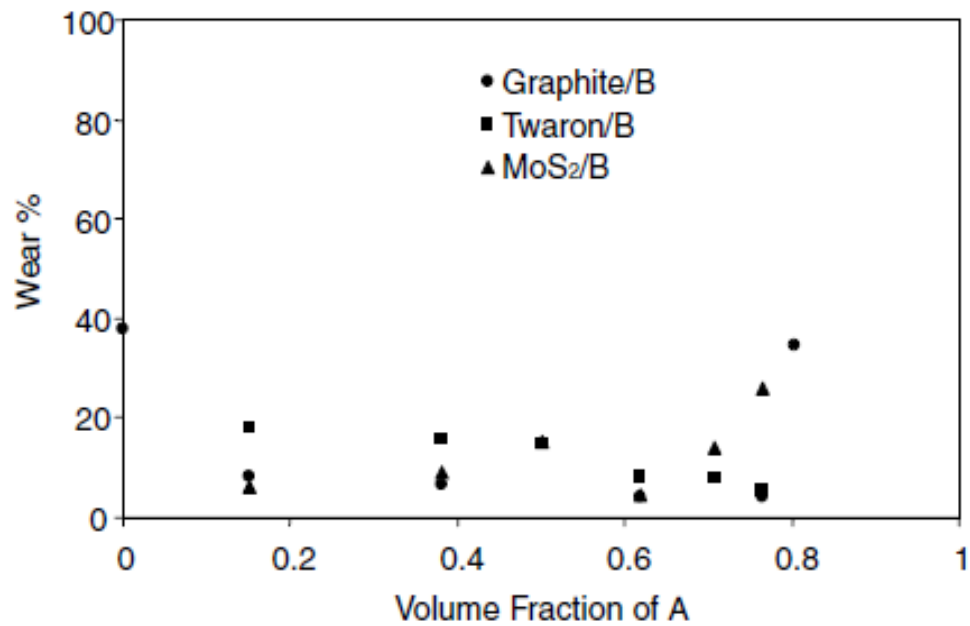
Figure 3.3 Wear composition relationships of hard matters/benzoxazine [50].
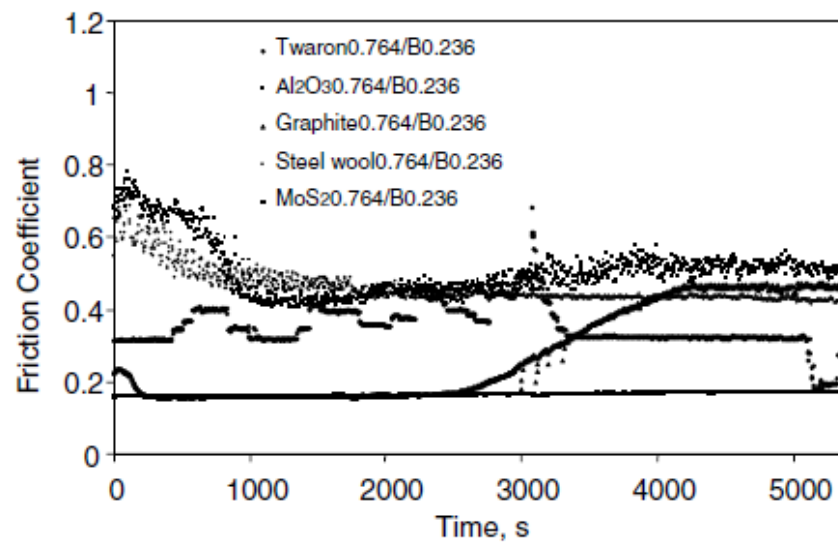
Figure 3.4 Wear composition relationships of soft matters/benzoxazine [50].

Nidhi and Bijwe [18] evaluated Nitrile Butadiene rubber (NBR) modified straight

phenolic resin on fade and recovery behavior of friction materials developed in the

laboratory. The friction materials were divided into two groups based on NBR-modified

phenolic resin and straight phenolic resin shown in Table 3.1. The author found value of fade in term fade% and coefficient of friction fade as follows, Fade μ: N_1 (0.259) > N_3 (0.242) > N_2 (0.228), S_1 (0.278) > S_2 (0.248) > S_3 (0.182) and % Fade: N_2 (26.45) > N_1 (22.91) > N_3 (21.42), S_3 (34.05) > S_2 (20.76) > S_1 (15.5). Furthermore the N_3 has shown greater tensile strength than other formulas because that composite comprised the most abundant of NBR in the composites. The authors concluded modification in straight phenolic resin by NBR improved tensile strength, thermal stability, friction performance and wear performance. If the composite increased amount of resin, higher was the wear rate and lower was the friction performance. The percent fade increased excessively with increase in amount of resin.

Table 3.1 Details about the 40% formulation of different composites (fixed percent by weight other fillers in composites) [18]

Types of series	Resins used in composites	Designation of the composites	Composition (weight percent)
Series N	NBR-modified phenolic resin	N_1	10
		N_2	12.5
		N_3	15
Series S	Straight phenolic	S_1	10
		S_2	12.5
		S_3	15

Nakamura et al. [51] investigated non-asbestos friction materials as brake pads, disc pads and various types of industrial equipment. The non-asbestos friction materials were produced by molding and curing a composition comprised of acrylonitrile-butadiene rubber-modified phenolic resin, a fibrous base, binder, and filler. The inventors have suggested the non-asbestos friction materials compositions made by providing a binder with the amount of the binder ca. 3 to 30wt%, wherein the acrylonitrile-butadiene rubber in the rubber-modified phenolic resin is from 10 to 40wt%. In addition, the amount of the fibrous base in the form of short fibers or a powder, i.e., inorganic fibers; aluminum fiber, potassium titanate fibers and organic fibers; aramid fibers, polyimide fibers, and acrylic fibers is 1 to 50wt%, and preferably 5 to 40wt%. The amount of the filler, i.e., inorganic fillers; calcium carbonate, barium sulfate, magnesium oxide, graphite, calcium hydroxide and organic fillers; cashew dust, nitrile rubber dust (vulcanized product) is 20 to 96wt%, based in on the overall weight of the friction material. The presented friction material compositions in this investigation showed in Table 3.2. The inventors have reported that the friction material has a 100 Hz vibration damping factor (tanδ) at 300°C minus tanδ at 50°C value of at least -0.030 which is advantageous for noise suppression. In addition, the resulting friction materials have an excellent and long-lasting noise performance, and good wear resistance, and fade resistance.

Table 3.2 Formulation of the friction materials [51].

Formulation	Ex8	Ex9
Aramid fibers	7	7
Glass fibers	7	7
Cashew dust	17	17
Calcium carbonate	13	13
Barium sulfate	21	21
Graphite	7	7
Copper powder	17	17
NBR-modified high-ortho phenolic resin	5.5	8.5
Acrylic rubber-modified Phenolic novolac resin	5.5	2.5
Total (% by weight)	100	100
Performance		
Short time modality	Good	Excellent
Noise performance	Good	Excellent
Functional stability	Excellent	Good
Fade resistance	Excellent	Good
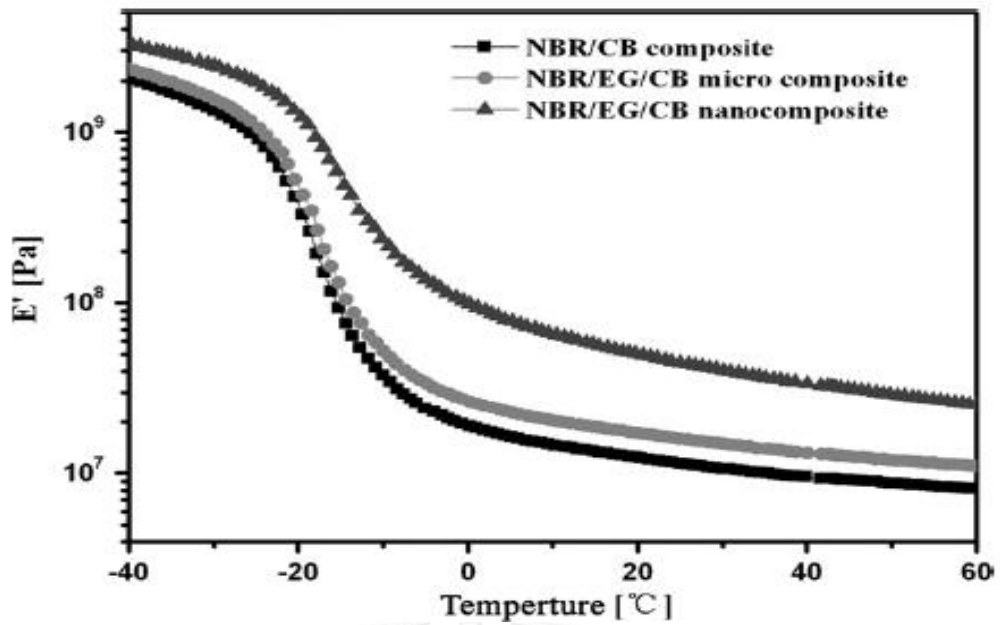
Figure 3.5 Storage modulus of composites [32].
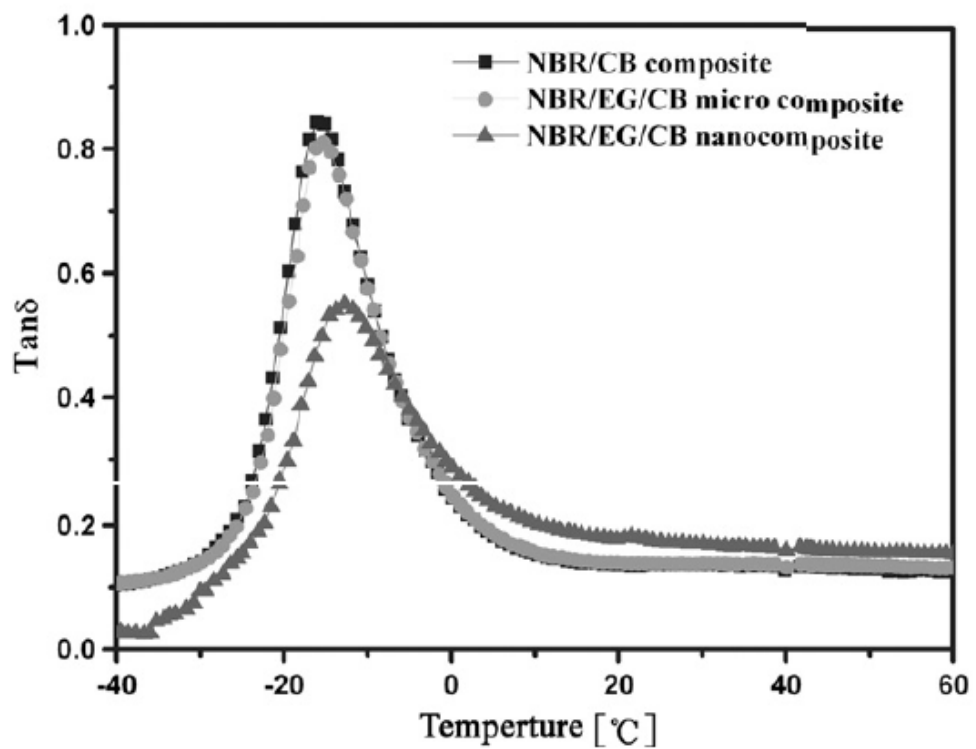
Figure 3.6 loss factor of NBR/CB and NBR/EG/CB composites [32]

Wang et al. [32] investigated mechanical and tribological properties of acrylonitrile–butadiene rubber filled with graphite and carbon black. In their work, acrylonitrile–butadiene rubber (NBR)/expanded graphite (EG)/carbon black (CB) micro- and nanocomposites were prepared by two different methods, and the resulting mechanical and tribological properties were compared with those of NBR/CB composites. Figure 3.5 and 3.6 displays the storage modulus (E_0) and loss factor (tanδ) as functions of temperature (from 40 to 60 °C). Similar to the results of the tensile properties, the E_0 of the NBR/EG/CB nanocomposite is higher than that of the other two composites. For nanocomposite, the hysteresis loss peak decreases, broadens and then increase resulting from the increase of effective filler volume fraction and a good graphite-rubber interface adhesion affected by nano-size dispersed graphite. The hysteresis loss of the composite resulted mainly from the viscoelasticity of rubber and filler–filler interactions. As discussed before, the mobility of the NBR macromolecular chains are restrained to some extent by nano-sized dispersed graphite sheets, which increases the effective volume fraction of filler and the relatively decreases the volume fraction of rubber, leading to the hysteresis loss decreases in glass transition region but increases in rubbery region. The wide loss peak indicates different mobility of rubber chains, whereas high storage modulus suggests good reinforcement. It can be also seen that the viscoelasticity of the NBR/EG/CB micro-composite changed little compared to the NBR/CB micro-composite.

The coefficient of friction (COF) and specific wear rate (W_s) values measured for NBR composites at different sliding velocities are illustrated in Figure 3.7 and 3.8 [32]. For all materials, the COF decreases with the increase of sliding velocity, a phenomenon called ''velocity weakening''. Note that EG has an obvious effect on the COF of NBR composites, especially at low sliding velocities (lower than 300 mm/s). In particular, the COF of the nanocomposite is the lowest of the three composites and is about 30% lower than that of the NBR/CB composite. The rate of decrease of COF with the sliding velocity increasing is the highest for the NBR/CB composite. As a result, at high sliding velocities (higher than 300 mm/s), the COF of NBR/CB composite is the lowest. In conclusion, EG is effective in reducing COF, and the effect of sliding velocity and graphite dispersion on COF is significant. From Figure 3.8, it can be noticed that the W_s of all composites decrease with the increase of sliding velocity. Under low sliding velocities, the W_s of the NBR/EG/CB nanocomposite is the lowest, while that of the NBR/CB composite is the lowest at high sliding velocities. These results are consistent with the trends of COF varied with sliding velocity, indicating that the COF is an important factor for wear rate [32].
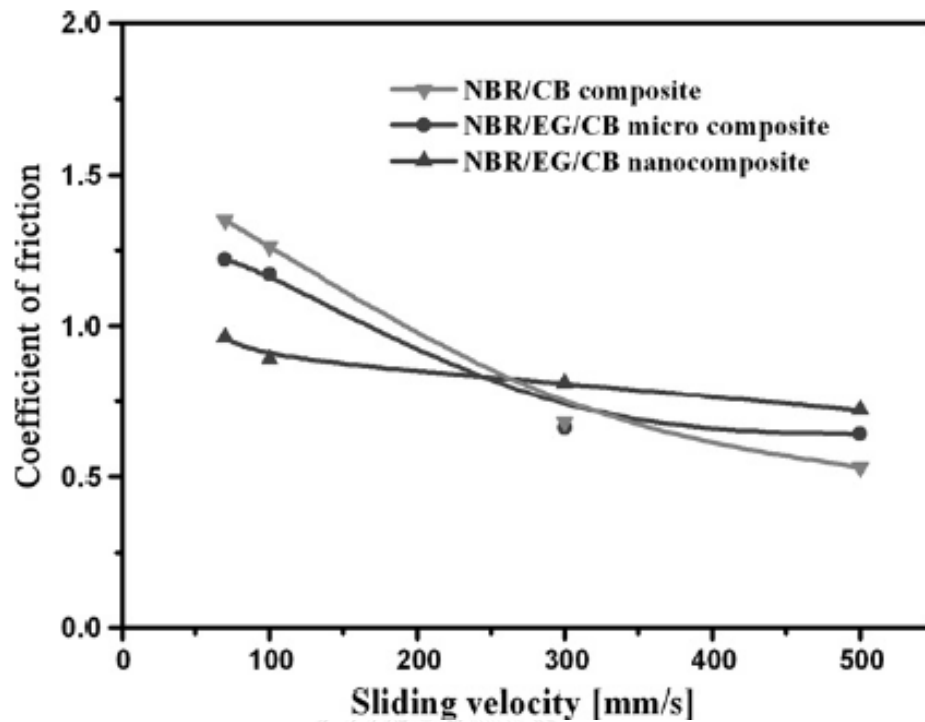
Figure 3.7 Effect of sliding velocity on coefficient of friction [32].

Saffar and Shojaei [52] studied effect of rubber component on performance of brake friction materials. The friction materials containing 40 % by volume organic binder (phenolic resin plus styrene-butadiene-rubber (SBR)) with varying phenolic-resin/SBR ratio were prepared. The content of phenolic resin in each composite was indicated by the resin value (RV) index ranging between 0 and 100% see in Table 3.3. The composites with RVs greater than 50% form resin-based friction materials in which the primary binder is the phenolic resin. For RVs less than 50%, the composites become the rubber-based materials where the primary binder is the SBR. The analysis of mechanical properties exhibited that the conformability of the composites increases upon incorporation of SBR. The frictional analysis revealed that type of polymeric

binder, i.e. resin or rubber, dominates greatly the frictional behavior of the composites. The increment of friction force and higher improvement in the frictional fade and recovery with sliding velocities are the general features of rubber-based friction materials. It was attributed to the inherent properties of rubber on the viscoelastic response at higher sliding velocities and entropic contribution on the mechanical properties at higher temperatures. The wear rate of resin-based materials and its drum temperature is lower than those of rubber-based materials as seen in Figure 3.9. It was attributed to the strongly adhered multilayer secondary plateaus formed on the surface of resin-based materials.
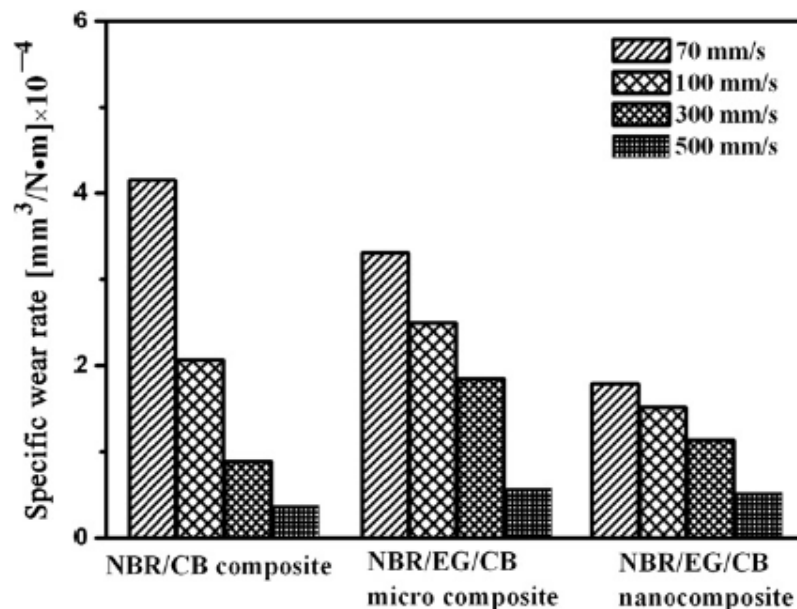
Figure 3.8 Wear rate of the composites (normal load is 60 N) [52].
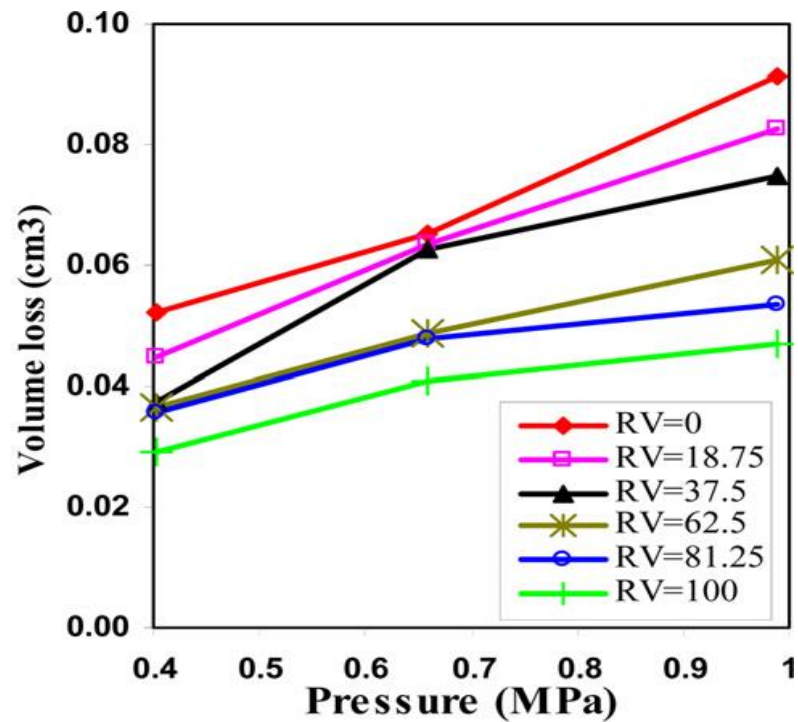
Figure 3.9 Wear of materials versus applied pressures at sliding velocity of 10.26 m/s [52].

Table 3.3 Formulation of the friction materials used in Saffar and Shojaei investigation [52].

Composition of friction materials	Resin-based compounds			Rubber-based compounds		
	PR-100	PR-81.25	PR-62.5	PR-37.5	PR-18.75	PR-0
Phenolic resin (vol.%)	40	32.5	25	15	7.5	0
Rubber component (vol.%)	0	7.5	15	25	32.5	40
Additives[a] (vol.%)	60	60	60	60	60	60
Total composition (vol.%)	100	100	100	100	100	100

Resin value of friction material (RV)[b]	100	81.25	62.5	37.5	18.5	0

[a] The additives include coal powder, graphite, calcium carbonate, iron powder, steel wool, barite, iron oxide, cashew dust, aramid pulp, vermiculite and alumina.

[b] Resin value (RV) defined here is the ratio of volume percent of phenolic resin per total volume percent of polymeric component (phenolic resin + rubber components which is 40 vol.% in all formulation) in percent.
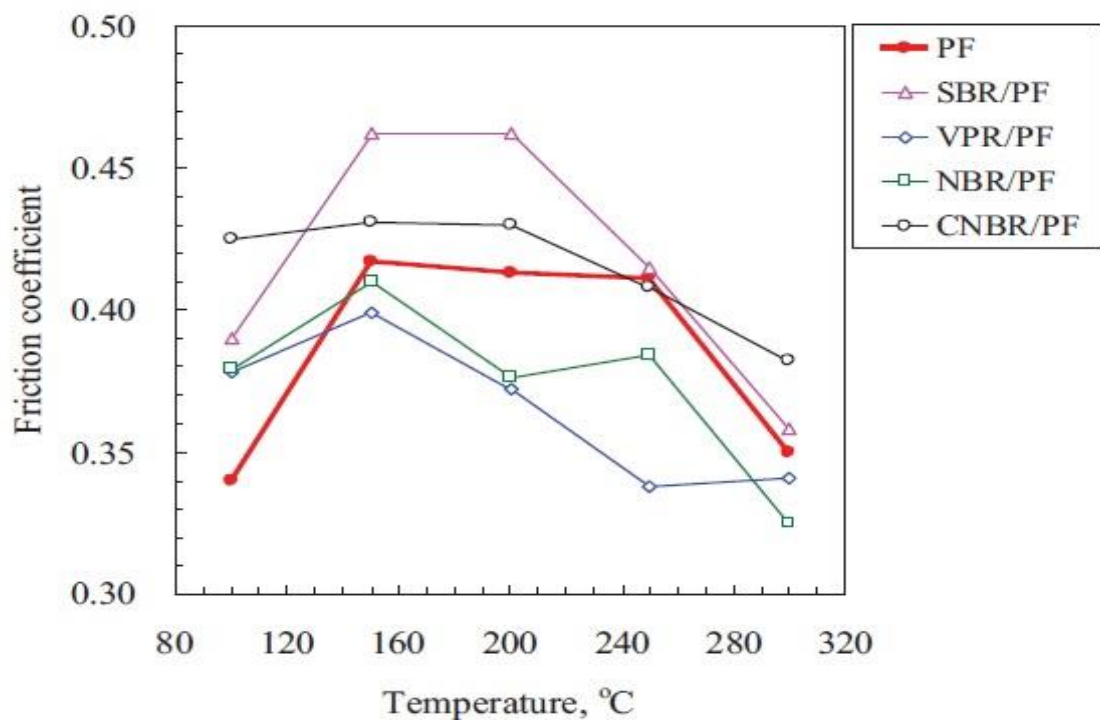
Figure 3.10 Friction coefficient of friction materials [19].

X. Liu et al.[19] studied vegetable oil modified phenolic resin (PF) blend with four types of rubber modifiers, i.e., styrene butadiene rubber (SBR) , styrene butadiene

2-vinyl pyridine rubber (VPR) , nitrile butadiene rubber, and carboxyl nitrile butadiene rubber (CNBR), were used as matrices for organic friction materials. Figure 3.10 presents the friction coefficient and wear rate as shown in Figure 3.11 of the organic friction materials at various temperatures. All the friction materials based on the rubber modified PFs showed higher friction coefficients compared with that based on the pure PF at 100°C. When the temperature was higher than 100°C, the friction coefficient of PF increased significantly, and the friction coefficients of the NBR/PF and VPR/PF materials were lower than that of the pure PF friction material. On the contrary, the friction coefficient of the SBR/PF and CNBR/PF friction materials remained higher than that of the pure PF based friction material. The CNBR/PF friction material exhibited the most stable friction coefficient at different temperatures, but had a value slightly below that of PF and SBR/PF at 240°C, but was higher than both at 280°C. The wear rate of all the friction materials increased with increasing temperature. When the temperature was higher than 200°C, the friction materials based on the rubber modified PFs all showed lower wear rate than the pure PF friction material. It is noteworthy that the wear rates of NBR/PF and CNBR/PF friction material were lower than that of the pure PF friction material at all temperatures, and the CNBR/PF friction material showed the lowest wear rate under all the testing temperatures.
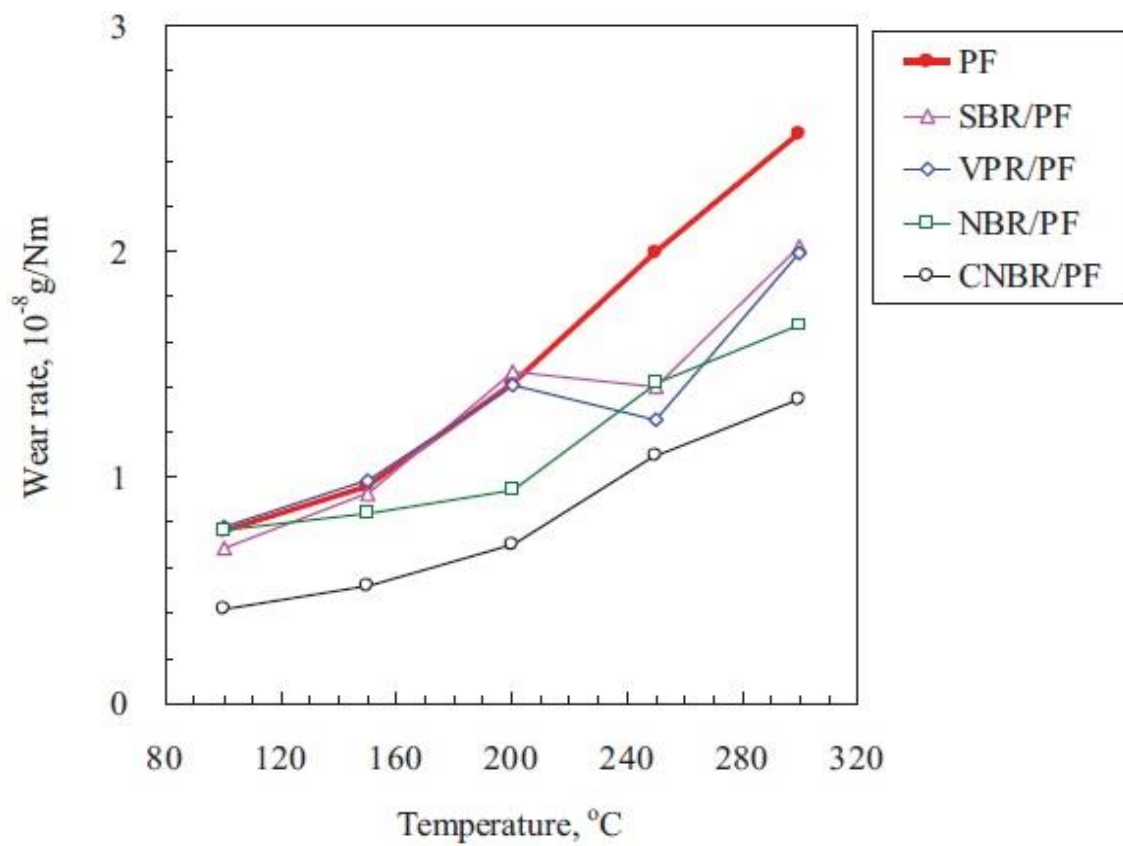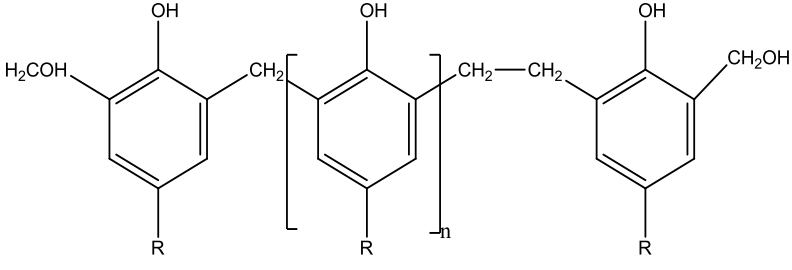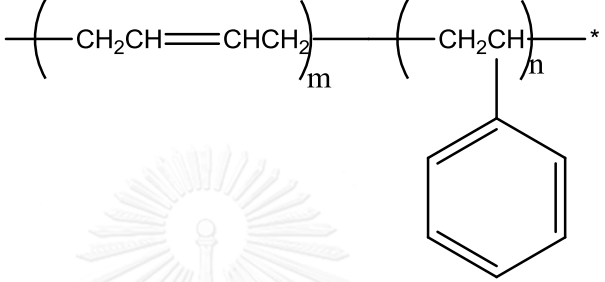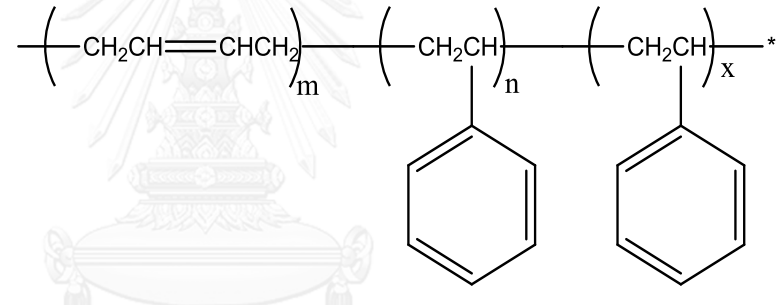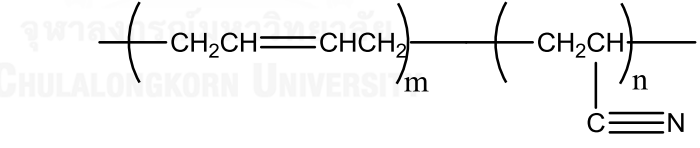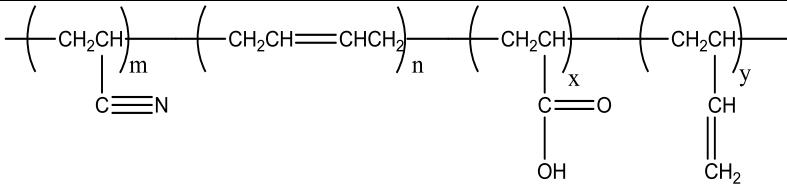
Figure 3.11 Wear rate of friction materials [19]

Figure 3.12 shows the wear of the brake pads after 36 cycles of braking tests. The wear of the NBR/PF and CNBR/PF pads was lower than pure PF pad, 0.87cm³/MJ, and lower than that of the required value of the China standard, 1.0 cm³/MJ. It is well known that excessively low wear behavior of a brake pad, however, is not good for the brake system because the pad should be a self-sacrificing material, or it may cause high wear of the matched metallic brake disc which is much more expensive than the organic brake pad.

Table 3.4 Chemical structure of the PF and the four rubber components [19]

Common name	Chemical structure
Phenolic resin	
styrene butadiene rubber	
styrene butadiene 2-vinyl pyridine rubber	
nitrile butadiene rubber	
carboxyl nitrile butadiene rubber	

Figure 3.12 Wear of the brake pads based on the pure PF, NBR/PF, and CNBR/PF pads after 36 cycles of braking tests. (load: 12.7 kN). [19]

Y. Wu et al. [55] investigated the effects of glass-to-rubber transition of thermosetting resin matrix on the friction and wear properties of friction materials. The friction materials were manufactured by mixing, hot press mounting, and post-curing. According to phenolic(PF), benzoxazine(BZ), phenolic resin/benzoxazine (P-B), and phenolic/benzoxazine/acrylonitrile-butadiene rubber (P-B-N) resin binders, the friction materials were coded as f-PF, f-BZ, f-P-B and f-P-B-N, respectively. The studied. Figure 3.13 shown the improved of glass transition temperature of the f-P-B composite when adding NBR in composite from $210^{\circ}C$ for f-BZ, 265 for f-PF and 265 for f-P-B increased to $290^{\circ}C$ for f-P-B-N. Furthermore, the addition of NBR can be increased friction

coefficient of the composite from 0.35 to 0.44 and improved friction stability at various

temperature from 100°C to 300°C of the composite as seen in Figure 3.14.
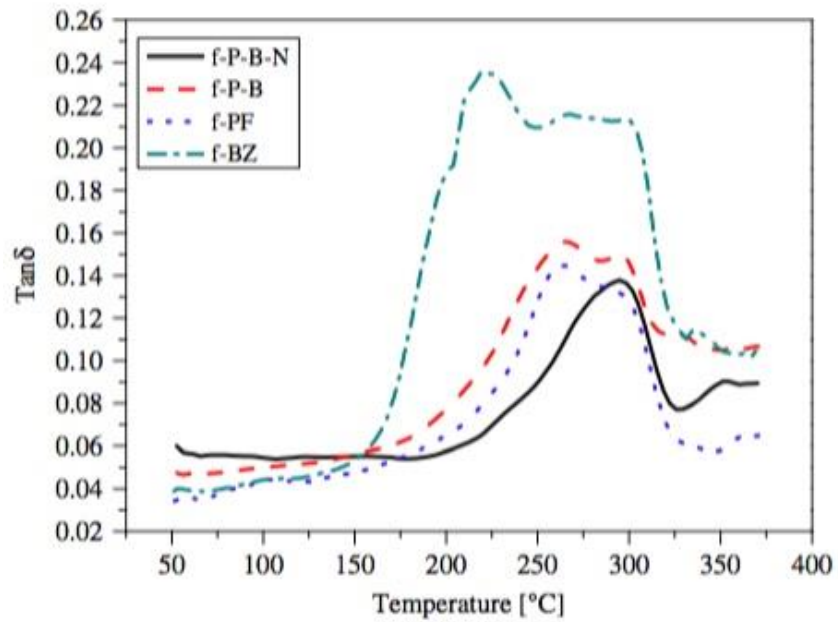
Figure 3.13 Tanδ as a function of temperature for resin based friction materials.[19]
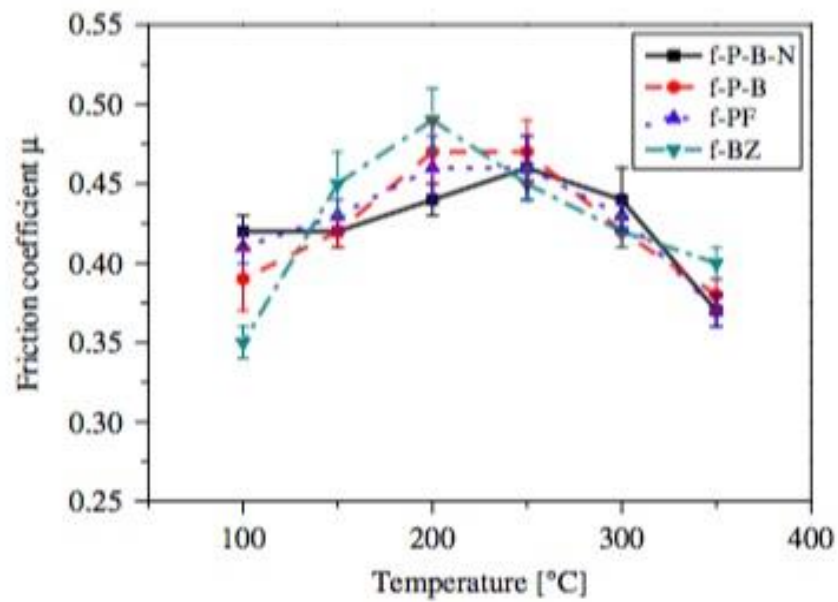
Figure 3.14 Friction coefficient as a function of temperature for resin based friction

materials. [19]

CHAPTER IV

EXPERIMENTAL

4.1 Materials and Monomer Preparation

The materials in this research are benzoxazine resin, micro- and ultrafine-acrylonitrile-butadiene rubber. Benzoxazine resin (BA-a) is based on bisphenol-A, aniline, and formaldehyde. PTT Phenol Co., Ltd. (TPCC) supplied the bisphenol-A (polycarbonate grade). Paraformaldehyde (AR grade) was purchased from Merck Company and aniline (AR grade) was obtained from Panreac Quimica SA Company. Micro-NBR (MNBR) has average particle size of 120 μm was purchased from Lanxess Emulsion Rubber Company and ultrafine-NBR (UNBR) has average particle size of 100 nm rubber was purchased from Sinopec Co., Ltd.

4.1.1 Benzoxazine Monomer Preparation

The benzoxazine resin used is based on bisphenol-A, aniline and formaldehyde in the ratio of 1:4:2 by mole. The resin was synthesized by using a patented solventless method in the U.S. Patent 5,543,516 (Ishida, 1996). The obtained benzoxazine monomer is clear-yellowish powder at room temperature and can be molten to yield a low viscosity resin at about 70-80 $^{\circ}$C. The product is then ground to fine powder and can be kept in a refrigerator for future-use. The density is 1.19 g/cm^3.

4.1.2 Acrylonitrile-Butadiene Rubber (NBR) Characteristics

Micro-NBR (MNBR) has particle size of 120 µm was purchased from Lanxess Emulsion Rubber Company and ultrafine-NBR (UNBR) has average particle size of 100 nm rubber was purchased from Sinopec Co., Ltd. Both MNBR and UNBR have bound acrylonitrile of 32.5 to 35.5 percent by mole.

4.2 Specimen Preparation

The rubber partilcles filled samples were prepared with MNBR or UNBR loadings of 0, 2, 5 and 15% by weight to yield molding compounds. The rubber was firstly dried at 80°C for 48 hours in an air-circulated oven until a constant weight was achieved and was then kept in a desiccator at room temperature. The filler was mechanically stirred to achieve uniform dispersion in benzoxazine resin using an internal mixer at about 110°C. For thermal-cured specimen, the compound was compression-molded by hot pressing. The thickness was controlled by using a metal spacer. The hot-press temperature of 200°C was applied for 3 hours using a hydraulic pressure of 10 MPa. All samples were air-cooled to room temperature in the open mold and were cut into desired shapes before testing.

4.3 Characterization Methods

4.3.1 Differential Scanning Calorimetric (DSC)

The curing characteristic of the benzoxazine-NBR composites were examined by using a differential scanning calorimeter (DSC) model DSC1 from Mettler-Toledo (Thailand) Ltd. For each test, a small amount of the sample ranging from 3-5 mg was placed on the aluminum pan and sealed hermetically with aluminum lids. The experiment using a heating rate of 10°C/min to heat the sealed sample from 30°C up to 300°C under N_2 purging. The purge nitrogen gas flow was constant at 50 ml/min. The processing temperature, time and glass transition temperature were obtained from the thermograms while the percentage of resin conversion was calculated from the DSC thermograms.

4.3.2 Density Measurement

4.3.2.1 Actual Density Measurement

The density of each specimen was determined by water displacement method according to ASTM D 792 (Method A). All specimens were prepared in a rectangular shape (50 mm $\times$ 25 mm $\times$ 2 mm). Each specimen was weighed in air and in water at $23\pm2^{\circ}$C. The density was calculated using Equation (4.1). An average value from at least five specimens was calculated.

$$\rho = \frac{A}{A-B} \times \rho_0 \qquad (4.1)$$

where ρ = density of the specimen (g/cm^3)

                A   = weight of the specimen in air (g)

                B   = weight of the specimen in liquid (water) at 23 ± 2°C (g)

                ρ_{o} = density of the liquid (water) at the given temperature (g/cm^3)

4.3.2.2 Theoretical Density Measurement

The theoretical density by mass of polybenzoxazine filled with rubber particles can be calculated as follow:

$$\rho_c = \frac{1}{\frac{W_f}{\rho_f} - \frac{(1-W_f)}{\rho_m}} \tag{4.2}$$

Where ρ_c = composite density, g/cm^3

                ρ_f = filler density, g/cm^3

                ρ_m = matrix density, g/cm^3

                ρ_c = composite density, g/cm^3

                W_f = filler weight fraction

                $(1-W_f)$ = matrix weight fraction

4.3.3 Dynamic Mechanical Analysis (DMA)

The dynamic mechanical analyzer (DMA) model DMA242 from NETZSCH Instrument was used to investigate dynamic mechanical properties. The dimension of specimens was 50 mm × 10 mm × 2.5 mm (W×L×T). The test was performed under the three-point bending mode. A strain in the range of 0 to 30 μm was applied sinusoidal at a frequency of 1 Hz. The temperature was scanned from 30 to 300°C with a heating rate of 5°C /min under nitrogen atmosphere. The glass transition temperature was taken as the maximum point on the loss modulus curve in the temperature sweep tests. The storage modulus (G$^{'}$), loss modulus (G$^{''}$), and loss tangent (tanδ) were then obtained. The glass transition temperature (T_g) was taken as the maximum point on the loss modulus curve in the DMA thermogram.

4.3.4 Thermogravimetric Analysis (TGA)

A thermogravimetric analyzer model TGA/SDTA 851^{e} from Mettler-Toledo (Thailand) was used to study thermal stability of NBR: polybenzoxazine composites. The initial mass of the composite to be tested was about 10 mg. It was heated from room temperature to 820°C at a heating rate of 20°C/min under nitrogen atmosphere. The degradation temperature at 5% weight loss and solid residue of each specimen determined at 800°C were recorded for each specimen.

4.3.5 Coefficient of friction Measurement

The friction behaviors of polybenzoxazine/NBR friction composites were evaluated using a pin-on-disc tribometer from CSM Instrument Ltd., Switzerland. The

dimension of samples was 27 mm in diameter and 6 mm in thickness. The friction tests were conducted at a linear speed of 36.6 cm/s and a load of 10 N for distance of 1000 m in temperature range of 25 to 250°C.

4.3.6 Wear Rate Measurement

The wear rate of all formulations of composites after sliding friction test was calculated by equation 2.1

$$W_s = [(W_1 - W_2) \times \frac{10^3}{\rho}]/Pvt \qquad (2.1)$$

Where W_s = the specific wear rate, mm^3/N·m

                W_1 = the weight before testing, g

                W_2 = the weight before testing, g

                ρ = composite density, g/cm^3

                P   = the applied normal load, N

                v = the relative sliding velocity, m/s

                t   = the experimental time, s

4.3.7 Scanning Electron Microscope testing

Worn surfaces obtained from sliding friction test was examined by using a JEOL JSM-5410 type scanning electron microscope. Fractographic studies were

especially used to determine possible rubber deformation mechanisms and distribution and interaction of rubber particles with the polybenzoxazine matrix.

CHAPTER V
RESULTS AND DISCUSSION

5.1 Characterization of Acrylonitrile-Butadiene Rubber (NBR) Particles filled Benzoxazine Resin Compounds

5.1.1 Curing Behaviors of Benzoxazine Resin (BA-a) Filled with Micro-NBR (MNBR) and BA-a Filled with Ultrafine-NBR (UNBR) Particles.

The curing behavior of benzoxazine resin (BA-a) filled with 0, 2, 5, 10 and 15wt% of micro-NBR (MNBR) particle detected by differential scanning calorimeter in a temperature range of 50°C to 300°C and at a heating rate of 10°C/min in nitrogen atmosphere is shown in Figure 5.1. From the figure, the exothermic peak of the neat BA-a observed at 220°C was attributed to the ring-opening polymerization of its oxazine-ring. The curing peak showed no significant shifting with an increase of MNBR particle contents. In addition, area under exothermic peak indicating the heat of reaction of the polymerization from monomer to polymer as seen in Figure 5.1 was increased with increasing of MNBR particle in the BA-a compounds. The values of area under exothermic peak increased from 277 J/g for the neat BA-a to 288, 294, 291 and 288 J/g for adding of MNBR particle at 2, 5, 10 and 15wt% to the BA-a compounds, respectively. This expected phenomenon related to the chemical reaction between the MNBR particle and the BA-a as it was observed from the increase of area under exothermic peak that the reaction between BA-a and NBR was explained by FT-IR analysis.

In similarity, the curing behavior of neat benzoxazine resin filled with 0, 2, 5, 10 and 15wt% of ultrafine-NBR (UNBR) particle contents was measured by differential scanning calorimeter in a temperature range of 50 to 300°C and at a heating rate of 10°C/min in nitrogen atmosphere is shown in Figure 5.2. Again, the addition of the UNBR particle showed no effect on the exothermic peak of the BA-a. In addition, area under exothermic peak indicating the heat of reaction of the polymerization from monomer to polymer as depicted in Figure 5.2 was increased with increasing UNBR particle in the BA-a compounds from 277 J/g for the neat BA-a to 285, 291, 288 and 290 J/g for adding UNBR 2, 5, 10 and 15wt%, respectively.

In addition, table 5.1 shows the calculated heat of reaction of BA-a/MNBR and BA-a/UNBR compounds. The heat of reaction was calculated by the difference of theoretical area under exothermic peak without reaction of BA-a and rubber particles and the actual area under exothermic peak. From the result, the difference of the heat of reaction between rubber particles was increased with increasing rubber particles content in the values of 17, 31, 42 and 53 J/g for BA-a filled with the MNBR particle of 2, 5, 10 and 15wt%, respectively, while that of BA-a/UNBR compounds filled with 2, 5, 10 and 15wt% UNBR particle was 14, 28, 39 and 55 J/g, respectively.

In term of curing condition, Figure 5.3 exhibited the DSC thermograms in a temperature range of 30°C to 300°C and at a heating rate of 10°C/min of 5wt% micro-NBR (MNBR)-filled benzoxazine resin compound cured at 200°C at curing time of 0, 1, 2 and 3 hours. In theory, the fully cured stage has been reported to provide a polymer

with desirable properties including sufficiently high thermal and mechanical integrity. From the figure, the heat of reaction of the uncured BA-a/MNBR (98/5) compound determined from the area under the exothermic peak was measured to be 288 J/g and the value decreased to 21, 8 and 6 J/g for curing times of 1, 2 and 3 hours, respectively, which corresponded to the degree of conversions estimated by Eq. (5.1) about 92.9, 97.3 and 97.9 after curing at 200°C for 1, 2 and 3 hours, respectively. The curing condition at 200°C for 2 hours was therefore used to cure all benzoxazine/NBR compounds to prepare the samples for further characterization.

$$\% \text{ conversion} = 1 - \frac{H_{rxn}}{H_0} \times 100 \qquad (5.1)$$

Where: H_{rxn} is the heat of reaction of the partially cured specimens.

           H_0 is the heat of reaction of the uncured resin.

5.1.2 Spectroscopic Property of Benzoxazine Resin (BA-a), Polybenzoxazine (PBA-a), Acrylonitrile-Buatadiene Rubber (NBR) and PBA-a/NBR composite

FT-IR spectroscopy was used to verify the molecular structures of benzoxazine resin (BA-a), polybenzoxazine (PBA-a), ultrafine acrylonitrile-butadiene rubber (UNBR) particle and 30wt% UNBR-filled PBA-a composite as plotted in Figure 5.4(a), 5.4(b), 5.4(c) and 5.4(d), respectively. The spectrum of UNBR exhibited the characteristic peaks at about 977 and 892 cm^{-1}, which is due to the trans-1,4 and 1,2-vinyl characteristic frequencies of the butadiene moieties due to out-of-plane

deformation of the =C-H, whereas the band at 2233 cm^{-1} is attributed to the −C≡N in

nitrile group. Furthermore, the figure shows FT-IR spectrum of PBA-a with a

characteristic peak at 1488 cm^{-1} due to tetra-substituted benzene ring that led to the

formation of a phenolic hydroxyl group-based polybenzoxazine (PBA-a) structure. In

addition, an indication of ring opening reaction of BA-a upon thermal treatment could

also be observed from the appearance of a broad peak about 3300 cm^{-1} which was

assigned to the phenolic hydroxyl group formation. The FTIR spectrum of the 30wt%

UNBR-filled PBA-a composite is presented in Figure 5.11(c). From this figure, though the

broad peak centered at around 3320 cm^{-1} due to the hydroxyl group was still observed,

its intensity tended to be lowered compared to those of the UNBR and the unfilled

polybenzoxazine implying the consumption of the −OH group in the polymer as well

as in the UNBR filler. In addition, the new peak at 1110 cm^{-1} assigned to C-O-C stretching

was also clearly observed in Figure 5.4(d). The appearance of this absorption band is

a clear evidence of the chemical bonding formed between the polybenzoxazine matrix

and the UNBR filler. According to Jubsilp et al., they investigated rubber-modified

polybenzoxazine composites for lubricating material applications. The authors used

the peak of C-O-C stretching at 1110 cm^{-1} to follow the formation reaction of ATBN

and polybenzoxazine composites from the starting benzoxazine resin and ATBN that

was reported by Jubsilp et al. [53]. Furthermore, The absorption band at 1640 cm^{-1}

typical of oscillations of the C=N group appears in the spectrum of the composite and

the intensity of the absorption band at 2233 cm^{-1} typical of oscillations of the C≡N

group diminishes that peak positions were reported by Kupreev [54].

5.2 Thermal and Mechanical Properties of Acrylonitrile-Butadiene Rubber (NBR)-filled
    Polybenzoxazine Composites

5.2.1 Dynamic Mechanical Analysis (DMA) of Micro-NBR (MNBR) filled
      polybenzoxazine and Ultrafine-NBR (UNBR) filled PBA-a

Since all polymers are viscoelastic in nature, dynamic mechanical analysis

method is suitable to evaluate complex transition and relaxation phenomena when

polymeric materials are presented. Figures 5.5 to 5.8 illustrate dynamic mechanical

properties of the micro-NBR (MNBR) particle filled polybenzoxazine (PBA-a). They were

recorded by dynamic mechanical analyzer in the temperature range of 30 to 250°C. At

room temperature, Figure 5.5 shows the storage modulus (E′) of MNBR particle filled

PBA-a composites with the MNBR content ranging from 0 to 15wt%. It obviously seen

from the storage modulus (E′) curves at room temperature, the PBA-a/MNBR

composites have lower values of E′ than the neat PBA-a. The results indicate that the

PBA-a exhibited the highest storage modulus at room temperature of 5.2 GPA, while

the content of MNBR particle in composites at 2, 5, 10 and 15wt% provided a storage

modulus values of 4.3, 3.7, 3.4 and 2.7 GPA, respectively. In addition, the results are

according to storage modulus of PBA-a/UNBR experiments.

Figure 5.6 exhibits loss modulus (E″) curves of MNBR particle filled

polybenzoxazine as a function of temperature. The maximum peak temperature in the

loss modulus curve was assigned as a glass transition temperature (T_g) of the specimen. As seen in the inset of this figure, the linear relationship between the glass transition temperature and the filler content was clearly observed. The glass transition temperature of the neat polybenzoxazine was determined to be 174°C whereas the glass transition temperature of the 15% by weight of MNBR particle filled polybenzoxazine is about 186°C. This phenomenon may be due to strong interfacial adhesion between the MNBR filler and the polybenzoxazine matrix as previously reported by Wu et al. [55] and certain chemical reaction of rubber particles and polybenzoxazine as reported by Kaynak et al [56].

In the part of ultrafine acrylonitrile-butadiene rubber (UNBR) particle filled polybenzoxazine (PBA-a) composites with the UNBR particle content ranging from 0 to 15wt% and records during dynamic mechanical analysis in the temperature range of 30 to 250°C is shown in Figure 5.7. This experiment had the same trend as PBA-a/MNBR composites. All formulations of the PBA-a/UNBR composites possess lower values of E´ than that of neat PBA-a. The results reveal that the PBA-a presented the highest storage modulus at room temperature of 5.2 GPA, while the content of UNBR particle in composites at 2, 5, 10 and 15wt% provided a storage modulus values of 4.5, 3.7, 3.1 and 2.6 GPA, respectively.

Loss modulus (E″) curves of UNBR-filled PBA-a with the UNBR particle content ranging from 0 to 15wt% were investigated in the temperature range of 30 to 250°C as illustrated in Figure 5.8. From the figure, glass-transition temperatures (T_g) achieved

from the maximum peak of loss modulus curve of the UNBR particle filled PBA-a composites were reported. The T_g values of the composites were observed to be in the range of 172°C to 188°C which were higher than that of the neat PBA-a as reported to be 172°C. Furthermore, the content of UNBR in composites at 2, 5, 10, 15 weight percent provided a glass-transition temperature values of 174, 176, 182 and 188 °C, respectively As the results, it could be seen that the T_g values systematically increased with increasing of UNBR contents in the composites. This phenomenon may be due to strong interfacial adhesion and chemical recation between the UNBR particulate filler and the polybenzoxazine matrix as previous discussion.

5.2.2 Thermal Degradation of Polybenzoxazine (PBA-a) Filled with Micro-NBR (MNBR) and PBA-a Filled with Ultrafine-NBR (UNBR)

Degradation temperature (T_d) is one of the important parameters used to determine temperature stability of polymeric materials. Figure 5.9 and 5.10 exhibits TGA thermograms of the neat polybenzoxazine and NBR particulate fillers filled polybenzoxazine composites at various NBR particle contents and sizes which included ultrafine-NBR (UNBR) and micro-NBR (MNBR) particles from 30 to 800°C at a heating rate of 20°C/min in nitrogen atmosphere. It was observed that pure MNBR particle exhibits outstandingly high thermal stability with only 5% total weight loss up to 374°C as seen in Figure 5.9. On the other hand, the polybenzoxazine matrix possesses a degradation temperature at its 5% weight loss of 325°C and the char residue at 800°C of 25%. From the thermograms, the degradation temperature at 5% weight loss of the

MNBR particulate filler filled polybenzoxazine composites systematically decreased with increasing MNBR particle content as seen in Figure 5.9 according with UNBR particulate filler filled polybenzoxazine composites as seen in Figure 5.10. The thermal resistance of the composite is lower than that of the PBA-a. This data confirm the conclusion on the formation of intermediate compounds during the mixing of rubber particle and PBA-a with a lower thermal resistance, which was drawn based on an analysis of the IR spectra as reported by Kupreev [54].

5.3 Friction and Wear Properties of Acrylonitrile-Butadiene Rubber (NBR)-filled Polybenzoxazine (PBA-a) Characterization

5.3.1 Coefficient of friction of Polybenzoxazine (PBA-a) Filled with Micro-NBR (MNBR) and PBA-a Filled with Ultrafine-NBR (UNBR)

Coefficient of friction (COF) or friction coefficient is a key parameter of friction materials that can be identified an application for the friction material. Figure 5.11 shows the COF at the room temperature with linear velocity of 36.6 cm/s and applied load of 10 N at 1000 meter in distance of MNBR-filled and UNBR-filled PBA-a composites with the MNBR and UNBR particles content ranging from 0 to 15wt%. From the results, it was found that MNBR and UNBR particles can improve COF of the PBA-a composites. The COF values of the UNBR composites were about 0.50, 0.54, 0.60, 0.61, and 0.62 for the addition of UNBR particle contents of 0, 2, 5, 10, and 15wt%, respectively. Moreover, the COF values of the PBA-a/MNBR composites were also increased from 0.50 for PBA-a to 0.61 for PBA-a/15wt% MNBR. This characteristic can

be explained that the COF generally increases with an increase of actual contact area and surface roughness due to an addition of the rubbers particles. In addition, the COF values of the composites were increased rapidly in the range of UNBR and MNBR particle contents from 0 to 5wt%. It is possible to have good dispersion of rubber particles in the PBA-a matrix. However, the addition of the NBR particles over than 5wt% shows the slightly increase of COF values assuming to the increased rough surface of the composites although the agglomeration occurred on composite surfaces at 10, and 15wt% of rubber particles content. Consequently, the actual contact area between pin surface and the composite surface is reduced for the PBA-a filled with 10 and 15wt% of NBR particles. This phenomenon was supported by SEM experimental section. Moreover, the relation of storage modulus and COF is shown in Figure 5.12. From the figure, under the same applied load, friction composites with relatively lower storage modulus were deformed easily, and had relatively larger real contact area between friction pairs, which resulted in relatively higher friction force and COF. To study the effect of temperatures on the COF of the composites, Figure 5.13 shows COF of the 5wt% UNBR-filled PBA-a composite at temperature range of 25 to 250°C with linear velocity of 36.6 cm/s and applied load of 10 N at 1000 m distance. From the figure, the composite presented a good stability of COF at various temperature because the COF of the composite can maintain in the rage of 0.51 to 0.60 [55].

5.3.2 Specific Wear Rate of Polybenzoxazine (PBA-a) Filled with Micro-NBR (MNBR) and PBA-a Filled with Ultrafine-NBR (UNBR)

The specific wear rate at room temperature after sliding test of 1,000 m calculated by Eq. (2.1) of MNBR-filled PBA-a and UNBR-filled PBA-a composites as a function of the NBR content was plotted in Figure 5.14. The specific wear rate values of the composites were about 3.35×10^{-4}, 2.50×10^{-4}, 1.83×10-4, 2.10×10^{-4}, and 3.11×10^{-4} mm^3/Nm for the addition of UNBR particle contents of 0, 2, 5, 10,;/ and 15wt%, respectively. In the case of MNBR-modified PBA-a composites, the specific wear rate was in the values of 3.35×10^{-4}, 2.70×10^{-4}, 2.10×10^{-4}, 2.38×10^{-4}, and 3.21×10^{-4} mm^3/Nm for the addition of MNBR particle contents of 0, 2, 5, 10 and 15wt%, respectively. It can be seen that PBA-a filled with 2wt% and 5wt% of rubber particles showed slightly lower specific wear rate than that of the neat PBA-a. This phenomenon is due to improved toughness and anti-cracking of the composites. In contrast, the specific wear rate were increased with increasing the rubber particles over than 10wt%. This can be explained by the agglomeration of the rubber particles in the PBA-a matrix as previously observed in phenolic/CTBN/nano-clay system [57] and PBA-a/ATBN copolymers [53].

Furthermore, table 5.2 shows the specific wear rate calculated by Eq. (2.1) after sliding test of 1,000 m of the PBA-a filled with 5wt% of UNBR as a function of temperature in the temperature ranges of 100 to 250°C. From the result, the specific wear rate of the composites was increased with increasing sample temperature from

$1.83×10^{-4}$ mm^3/Nm to $4.61×10^{-4}$, $12.07×10^{-4}$, $51.07×10^{-4}$, and $102.33×10^{-4}$ mm^3/Nm at

the temperatures of 25, 100, 150, 200 and 250℃, respectively. The specific wear rates

of all friction composites gradually increased with an increase of temperature to 150℃,

and then increased dramatically when temperature was above 200℃. This behavior is

due to the thermal decomposition effect of the resin binders above 250℃, resulting

in increasing of specific wear rate and reduction in COF as above mentioned.

$$W_s = [(W_1 - W_2) \times \frac{10^3}{\rho}]/Pvt \qquad (2.1)$$

Where

W_s (mm^3/N·m)   = the specific wear rate

W_1 (g)   = the weight before test

W_2 (g)   = the weight after test

ρ (g/cm^3)   = the density of sample

P (N)   = the applied normal load

v (m/s)   = the relative sliding velocity

t (s)   = the experimental time

5.3.3 SEM of UNBR-Filled Polybenzoxazine (PBA-a) Composites

Figures 5.15(a) to 5.15(e) show the worn surface of the neat PBA-a and the

UNBR-filled PBA-a composites with sliding velocity of 0.366 m/s after distance of 1,000

meter at room temperature. SEM micrograph of the PBA-a is shown in Figure 5.15(a), it exhibited the brittle characteristic, and it could easily crack and break on the sample surface. These characteristics cause an increase in a specific wear rate of the PBA-a. In cases of PBA-a filled with UNBR composites, the worn surface of PBA-a filled with UNBR particle of 2wt% and 5wt% exhibited in Figures 5.15(b) and 5.15(c), respectively. It can be seen that the PBA-a filled with 2wt% and 5wt% of UNBR particles shows a good dispersion of the UNBR particles in the PBA-a matrix, and the worn surface of the composites was attributed to the fine cracking and deformation, resulting in an increase in the COF of the composites due to their higher friction force developed at the interface. Thus, the deformed rubber particles on the composite surface play protective role against the wear damage to the composites as previously reported that a small amount of the UNBR particle contributed to a reduction of the specific wear rate as shown in Figure 2. Furthermore, the addition of UNBR particles in the PBA-a was found to reduce the surface cracking on the composite surface. In contrast, the agglomeration of the UNBR particles was observed for the composite filled with the UNBR particle more than 5wt% as can be seen in Figures 5.15(d) and 5.15(e), resulting in an increase of the specific wear rate on the PBA-a filled with 10wt% and 15wt% of UNBR particle.

Moreover, the worn surface with sliding velocity of 36.6 cm/s after distance of 1,000 meter in the temperature range of 100 to 250°C of the PBA-a filled with 5wt% UNBR shows in Figure 5.16(a) to 5.16(d). From the figure, the effect of temperature on

the worn surface of the composite was investigated by scanning electron microscope

(SEM) with 100x magnification. It is well known that the raised of friction material

temperature that can be made more wear rate of the phenolic based friction material

as seen in table 5.2. The worn surfaces of the composite at 100 and 150°C as can be

seen in figure 5.16(a) and 5.16(b), respectively. It was observed that the rubber particles

was deformed and well dispersed in the PBA-a matrix. Figure 5.16(c) showed the worn

surface of the composite at 200°C which was a higher glass transition temperature of

the composite. COF section shown the low efficiency of COF because the polymer

chain of the matrix can be moving that is expected to the composite cannot fixed

maintain the shape for act as the highest performance like composite at 25, 100 and

150°C. Moreover, figure 5.16(d) showed the worn surface of PBA-a filled with 5wt% of

UNBR at 250°C. The figure shows that the thermal degradation of the composites

occurred in this temperature test as discussed in the COF section. Furthermore, The

testing temperature at 250°C refer to initial degradation temperature of the composite

therefore the composite surface was demolished during the friction test at this

temperature.

5.4 Suggested Brake Pads Formulation from Our Work

   5.4.1 Comparison of Phenolic Based Composites and PBA-a Based Composite for
         Brake Pads Application

         The formulation of the friction composite based on phenolic resin and

benzoxazine resin (BA-a) is followed by US Patent number 8,227,390 B2 [8] as listed in

Table 5.3. The curing condition to obtain the fully-cured composites was by heating at

200°C for 3.5 hours in a hydraulic hot-pressed machine at 15 MPa. Some essential

properties of brake pads application of phenolic based and polybenzoxazine based

are shown in Table 5.4. The flexural properties was determined using a universal testing

machine Instron model 5567 from USA. Flexural tests were performed on 1 cm thick

bar according to three-point bending method of ASTM D790. The PBA-a based

composite represents to the good mechanical properties i.e. storage modulus, flexural

modulus, and flexures strength with the value of 6.2 GPa, 6.4 GPa, and 61 MPa

respectively. It can be seen that those values have nearly twice of the phenolic based

composite. In term of the thermal properties, the glass transition temperature (T_g) and

thermal degradation temperature at 5 percent weight loss (T_{d5}) were investigated. The

T_g and the T_{d5} of the PBA-a based composite was similar to those of the phenolic

based composite. The T_g and T_{d5} was in the range of 210 to 215°C, and 410 to 424°C,

respectively. For tribology properties included coefficient of friction (COF) and specific

wear rate of the composites, the COF of the PBA-a based composite, i.e. 0.35 was

higher than that of the phenolic based composite, i.e. 0.29. Furthermore, the PBA-a

based composite showed the lower specific wear rate than the phenolic based resin.

This phenomenon suggested that the benzoxazine resin can totally wet and bind other
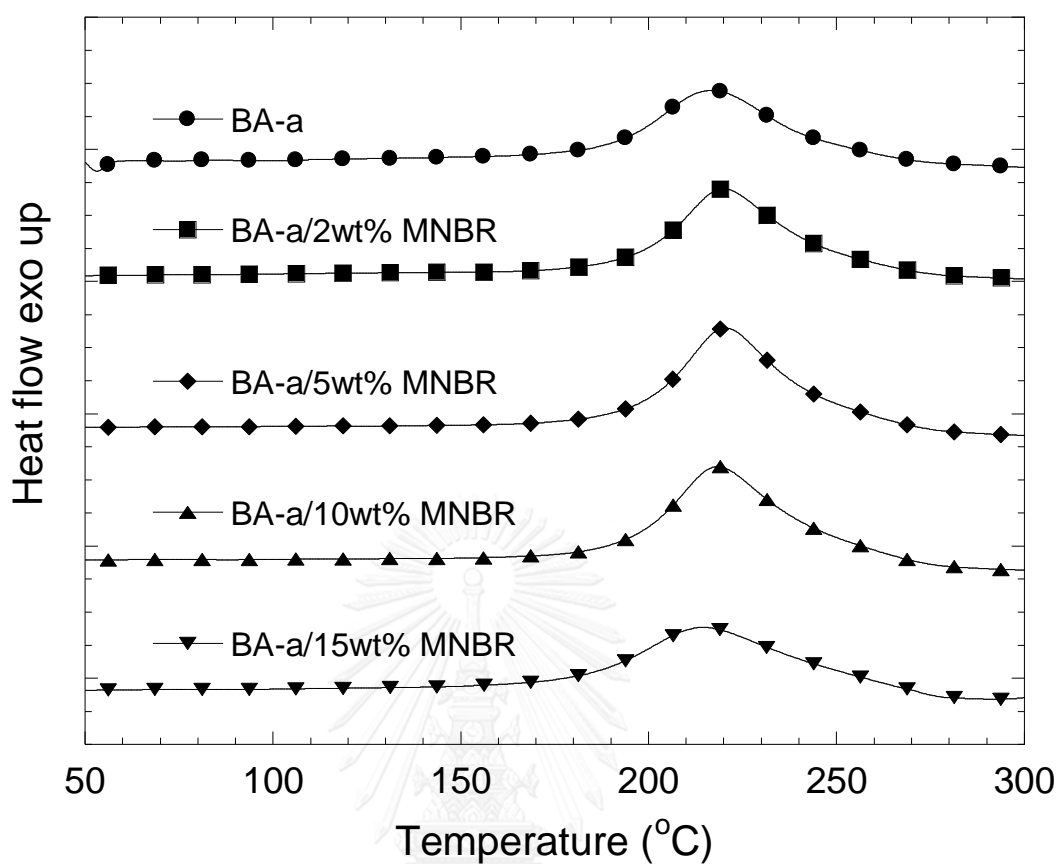
fillers in the composite.

Figure 5.1 DSC thermograms of benzoxazine molding compounds at different micro-

NBR (MNBR) contents: (●) neat benzoxazine monomer, (■) 2wt%, (♦)

5wt%, (▲) 10wt%, (▼) 15wt%.
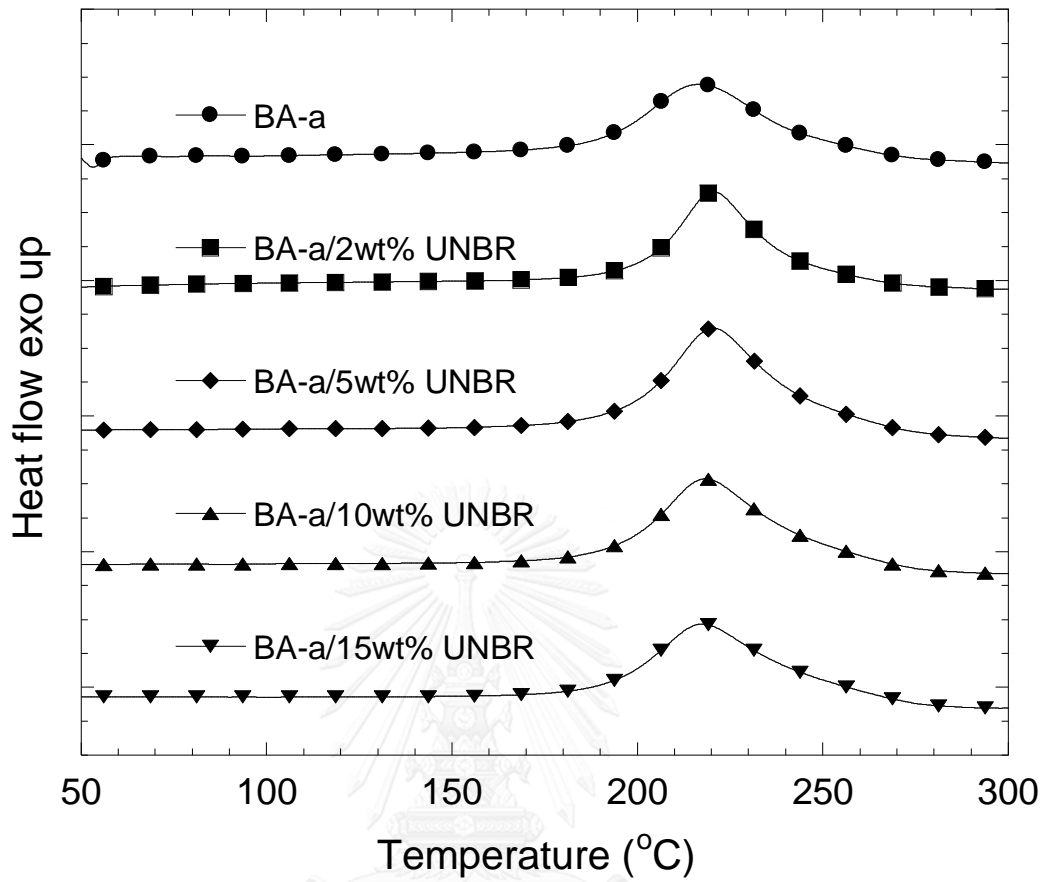
Figure 5.2 DSC thermograms of benzoxazine molding compounds at different

ultrafine-NBR (UNBR) contents: (●) neat benzoxazine monomer, (■) 2wt%,

(♦) 5wt%, (▲) 10wt%, (▼) and 15wt%.

Table 5.1 Approximate heat of reaction of molding compounds.

Rubber content (wt%)	Heat of reaction (J/g) of BA-a/UNBR	Heat of reaction (J/g) of BA-a/MNBR	Calculated heat of BA-a curing (J/g)	Calculated heat of UNBR react (J/g)	Calculated heat of MNBR react (J/g)
0	277	277	277	0	0
2	285	288	271	14	17
5	291	294	263	28	31
10	288	291	249	39	42
15	290	288	235	55	53
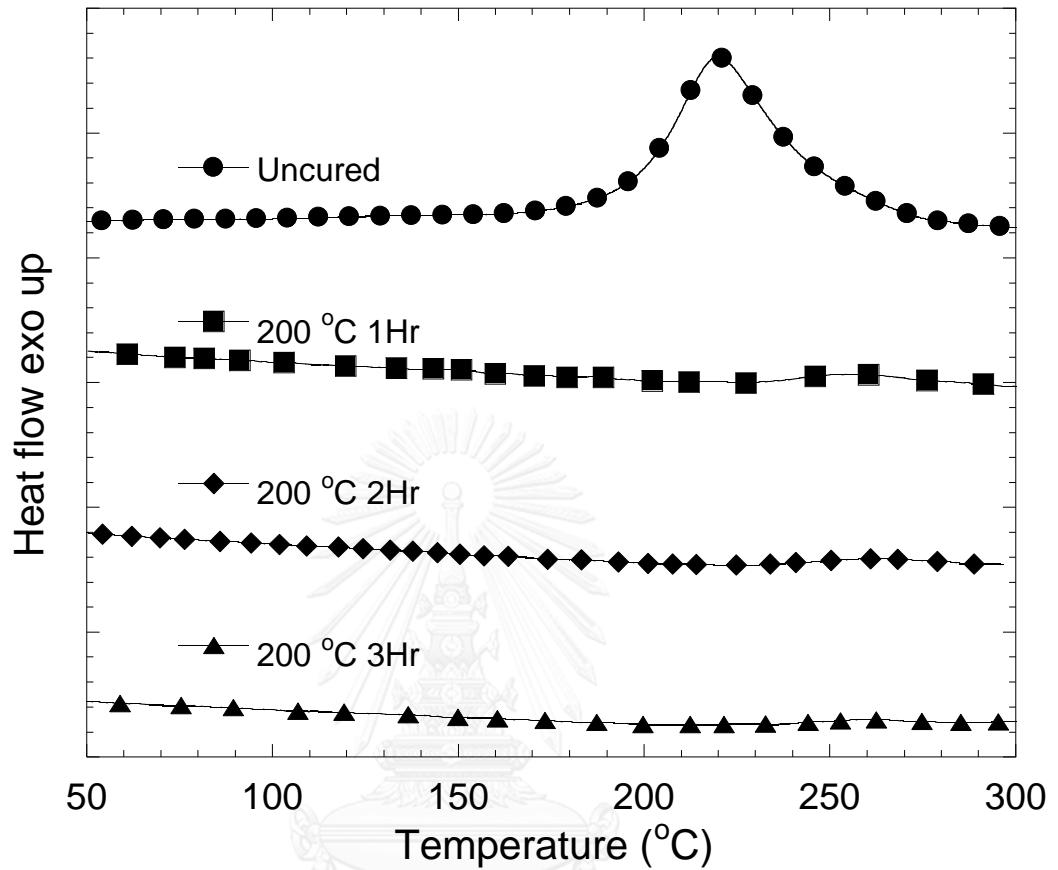
Figure 5.3 DSC thermograms of the composite (5wt% MNBR) at various curing times at 200°C: (●) Uncured molding compound, (■) 1 hour, (♦) 2 hours and (▲) 3 hours.
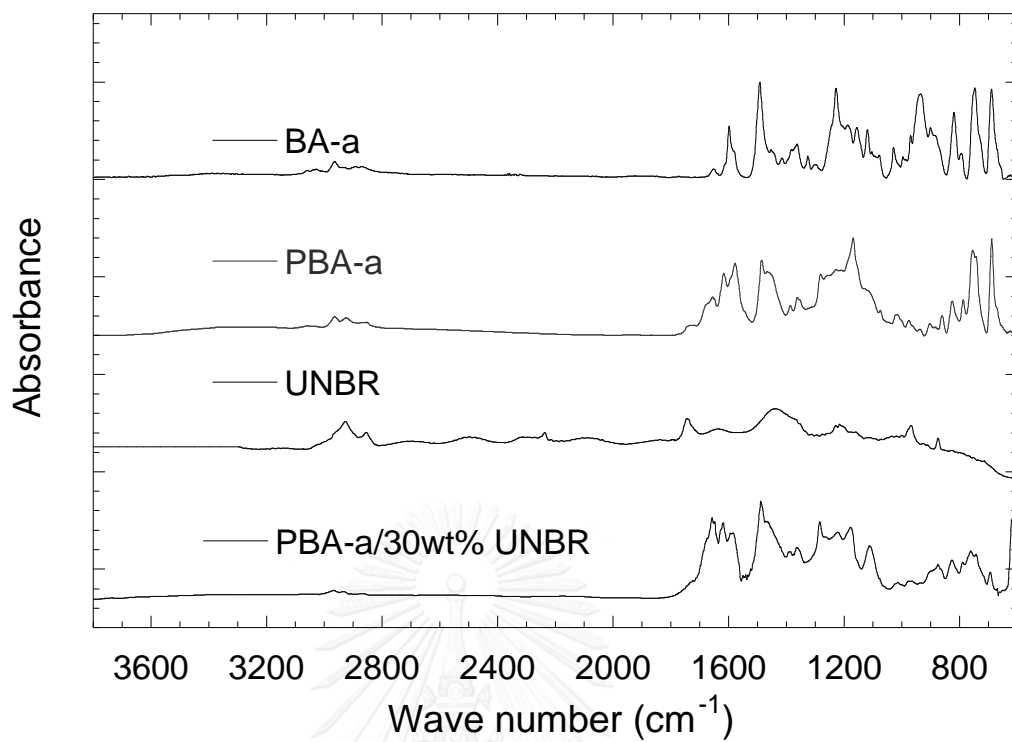
Figure 5.4 FTIR analysis of benzoxazine and compound (a) benzoxazine resin (BA-a)
(b) neat polybenzoxazine (PBA-a) (c) neat ultrafine-NBR (UNBR) and (d)
polybenzoxazine filled with 30wt% ultrafine-NBR (PBA-a/30wt% UNBR).

Figure 5.5 DMA thermograms of storage modulus of micro-NBR (MNBR) filled

polybenzoxazine composites: (●) neat polybenzoxazine (PBA-a), (■) 2wt%,
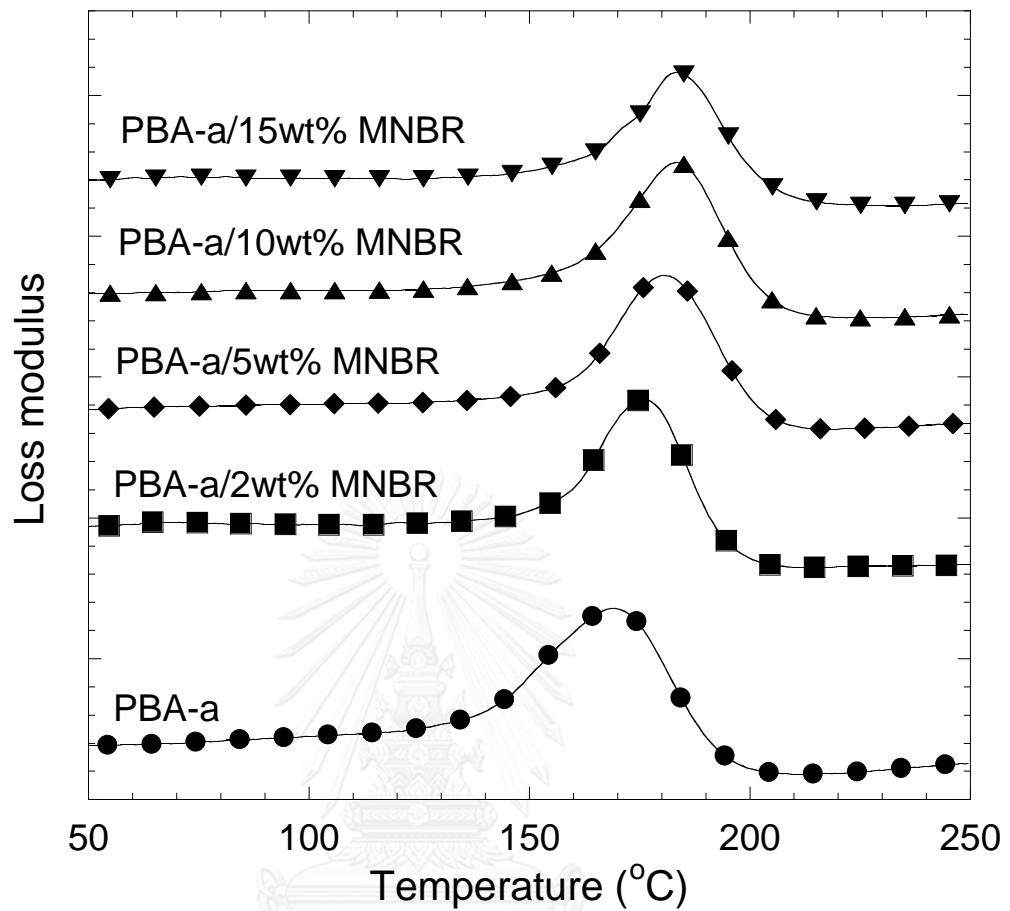
(♦) 5wt%, (▲) 10wt%, (▼) and 15wt%.

Figure 5.6 DMA thermograms of loss modulus of micro-NBR (MNBR) filled
polybenzoxazine composites: (●) neat polybenzoxazine (PBA-a) (■) 2wt%,
(♦) 5wt%, (▲) 10wt%, and (▼) 15wt%.
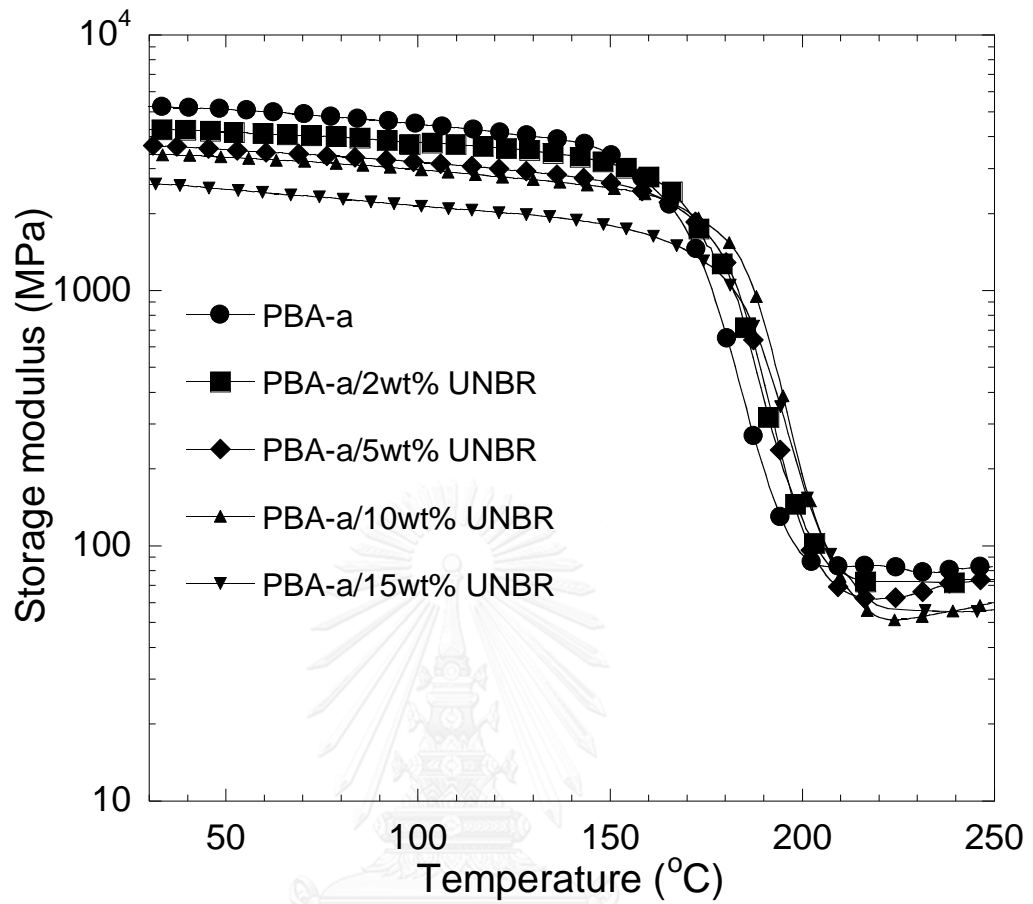
Figure 5.7 DMA thermograms of storage modulus of ultrafine-NBR (UNBR) filled

polybenzoxazine composites: (●) neat polybenzoxazine (PBA-a), (■) 2wt%,
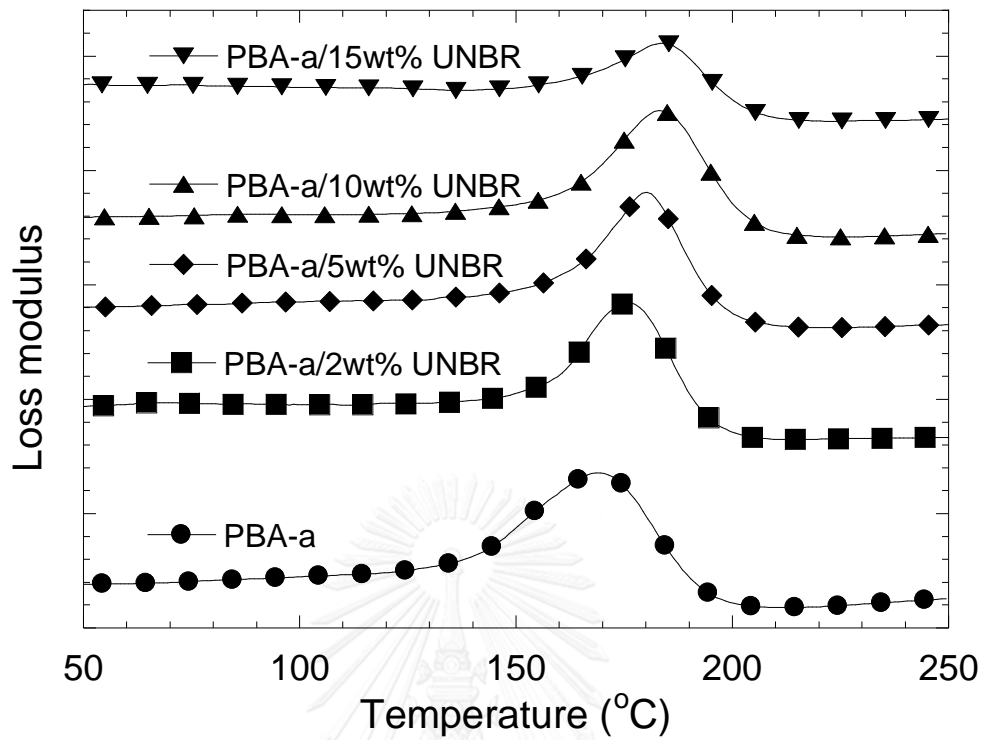
(♦) 5wt%, (▲) 10wt% and (▼) 15wt%.

Figure 5.8 DMA thermograms of loss modulus of ultrafine-NBR (UNBR) filled

polybenzoxazine composites: (●) neat polybenzoxazine (PBA-a), (■) 2wt%,
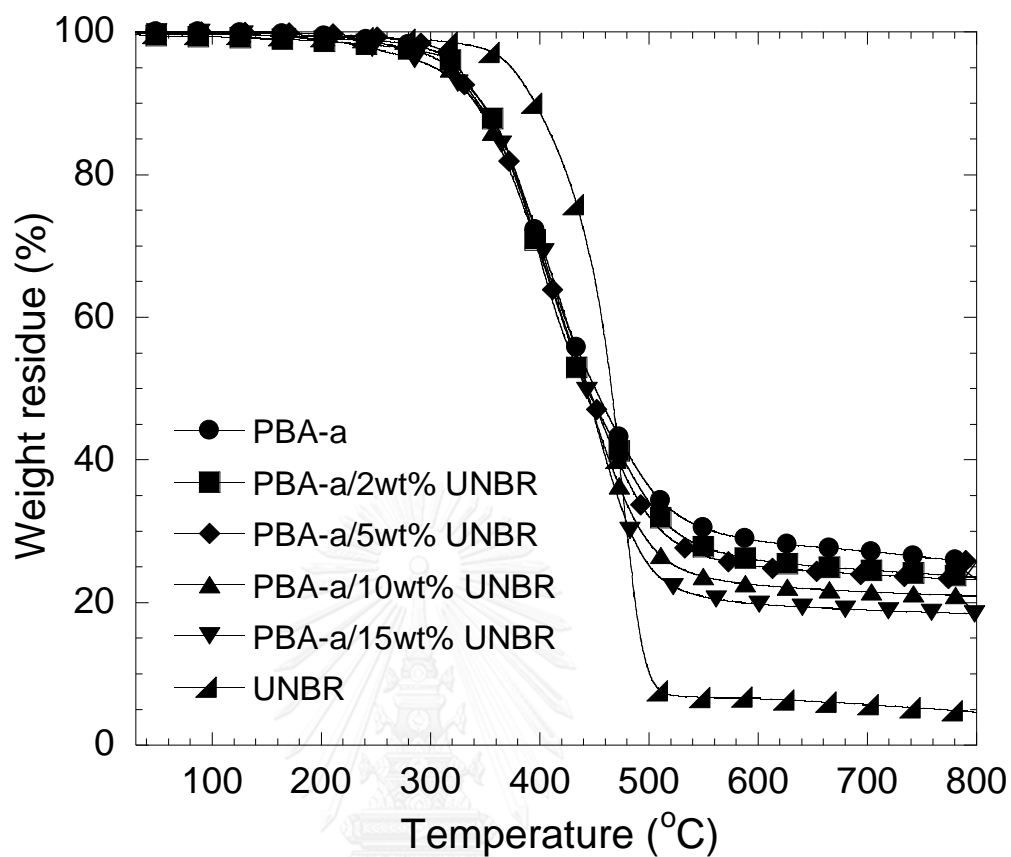
(♦) 5wt%, (▲) 10wt% and (▼) 15wt%.

Figure 5.9 TGA thermograms of MNBR filled polybenzoxazine composites: (●) neat

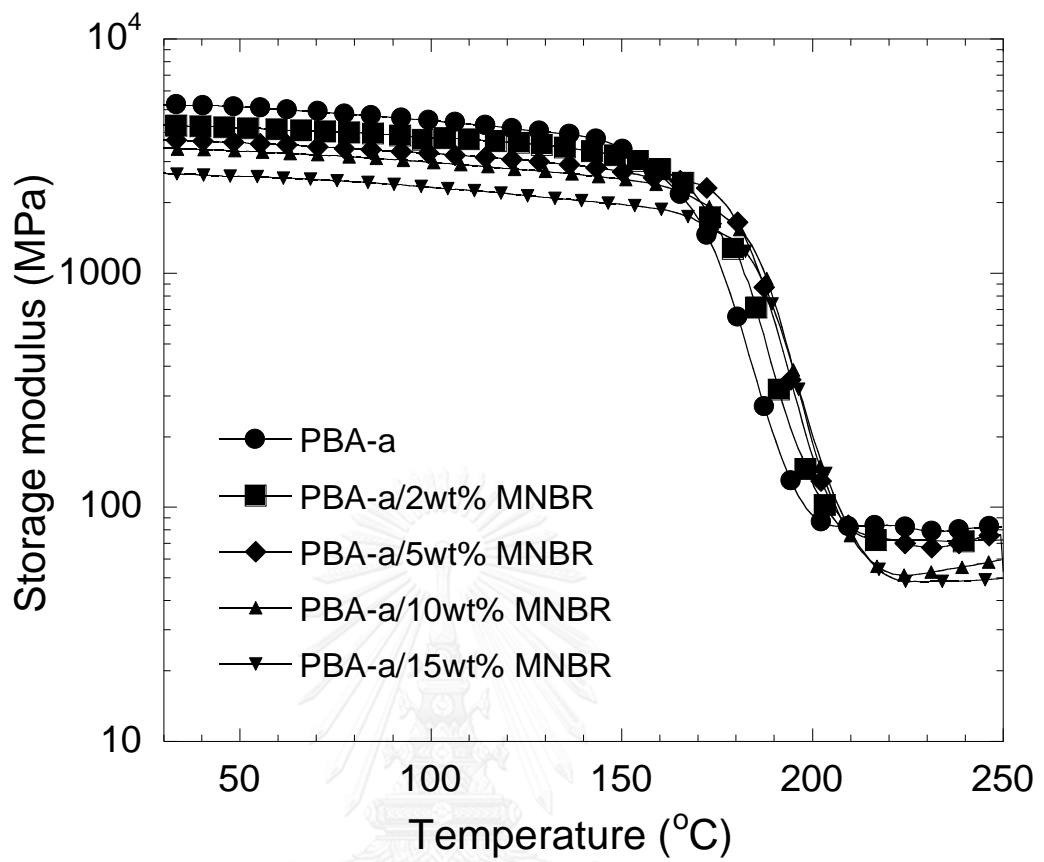polybenzoxazine (PBA-a) (■) 2wt%, (♦) 5wt%, (▲) 10wt%, (▼) 15wt%

and (◀) neat MNBR.
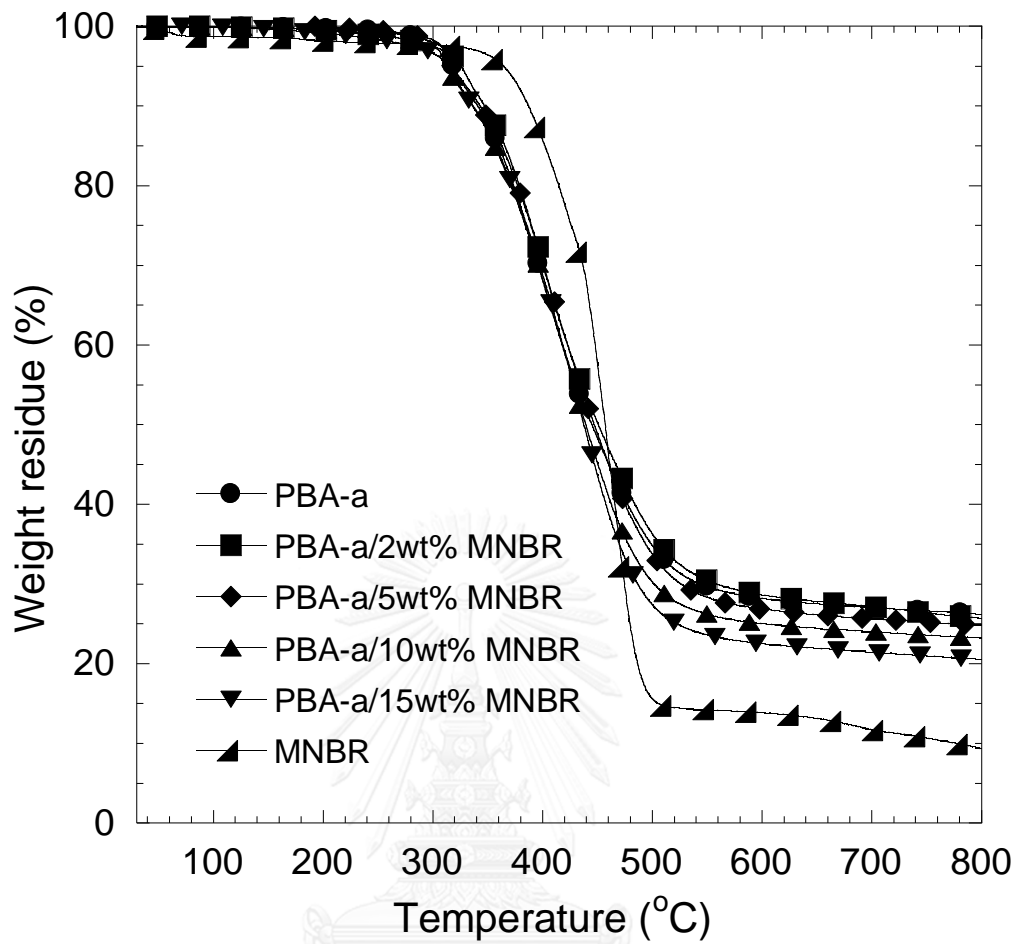
Figure 5.10 TGA thermograms of ultrafine-NBR (UNBR) filled polybenzoxazine

composites: (●) neat polybenzoxazine (PBA-a), (■) 2wt%, (♦) 5wt%,

(▲) 10wt%, (▼) 15wt% and (◄) neat UNBR.
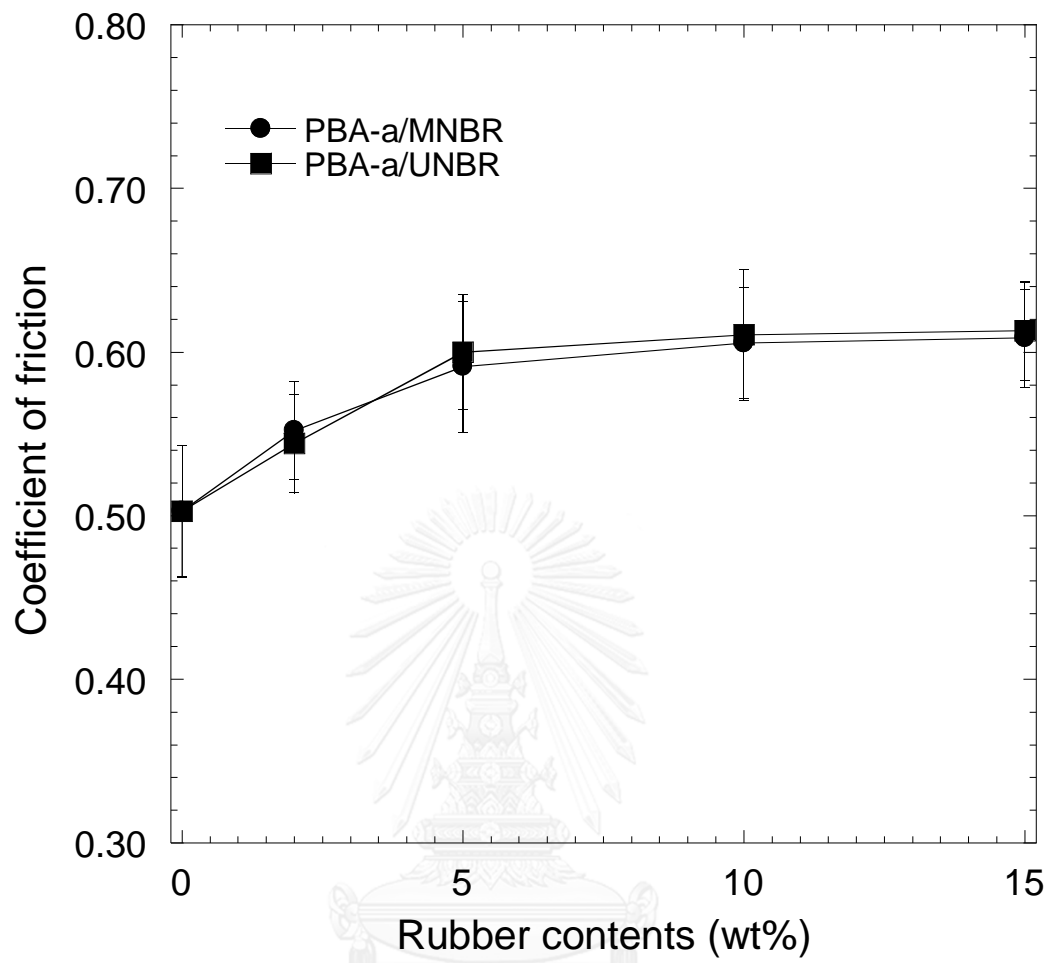
Figure 5.11 Coefficient of friction (COF) of polybenzoxazine filled with (●) micro-NBR
(MNBR) and (■) ultrafine-NBR (UNBR) with linear velocity of 36.6 cm/s and
applied load of 10 N in distance of 1000 m at room temperature.
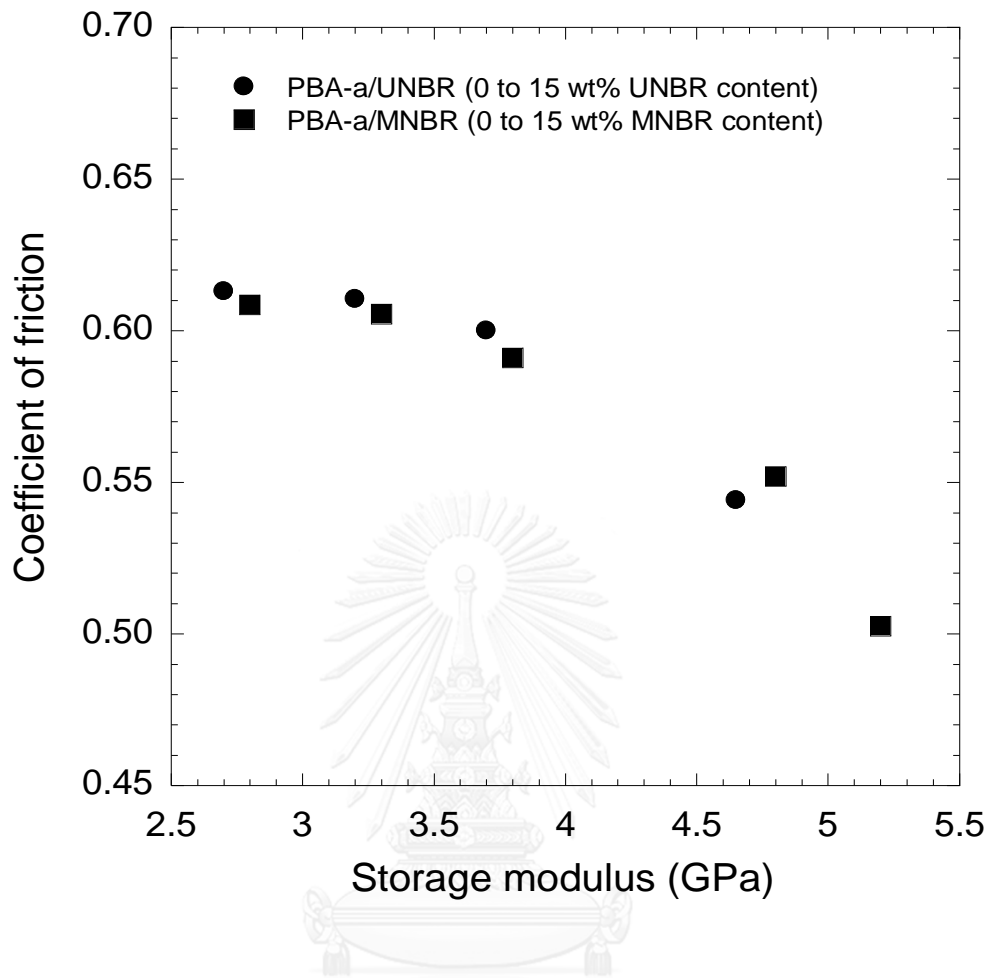
Figure 5.12 The relation between storage modulus and coefficient of friction of (●) micro-NBR (MNBR) and (■) ultrafine-NBR (UNBR) filled polybenzoxazine composites.
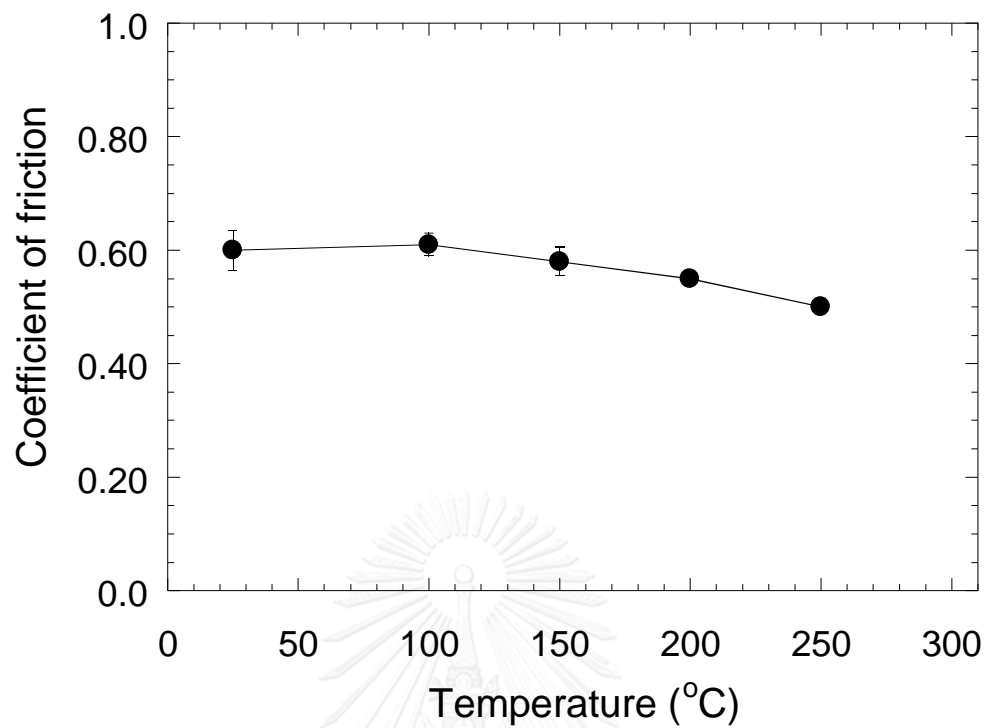
Figure 5.13 Coefficient of friction as a function of temperature of PBA-a filled with (●)

5wt% of ultrafine-NBR (UNBR) with linear velocity of 36.6 cm/s and

applied load of 10 N at 1000 m distance in temperature range of 25 to

250°C.
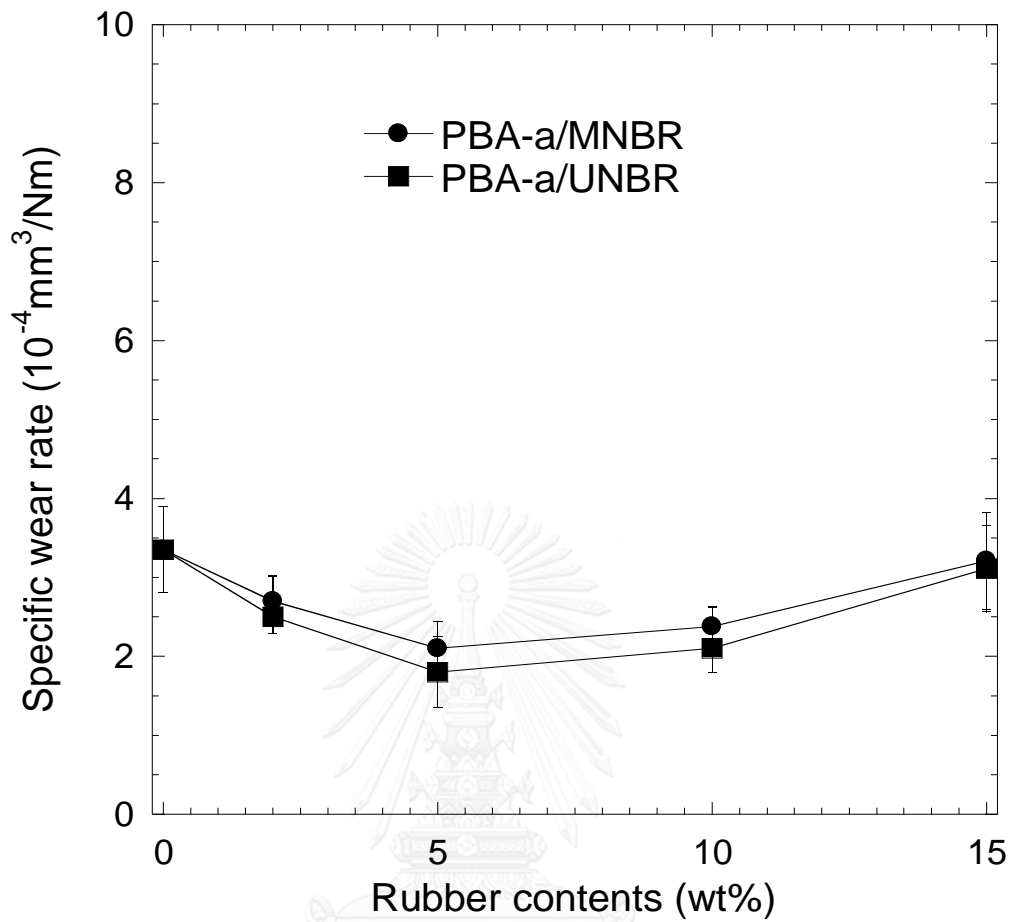
Figure 5.14 Specific wear rate of polybenzoxazine filled with (●) micro-NBR (MNBR) and (■) ultrafine-NBR (UNBR) with linear velocity of 36.6 cm/s and applied load of 10 N at 1000 m in distance at room temperature.

Table 5.2 Specific wear rate of polybenzoxazine filled with 5wt% of UNBR as a function of temperature in temperature range of 25 to 250°C

Testing temperature (°C)	Specific wear rate (10^{-4}×mm^3/Nm)
25	1.83±0.34
100	4.61±0.29
150	12.07±2.51
200	51.04±8.11
250	102.33±15.01
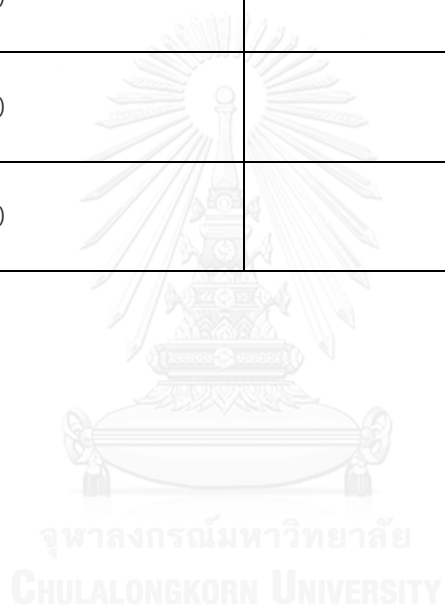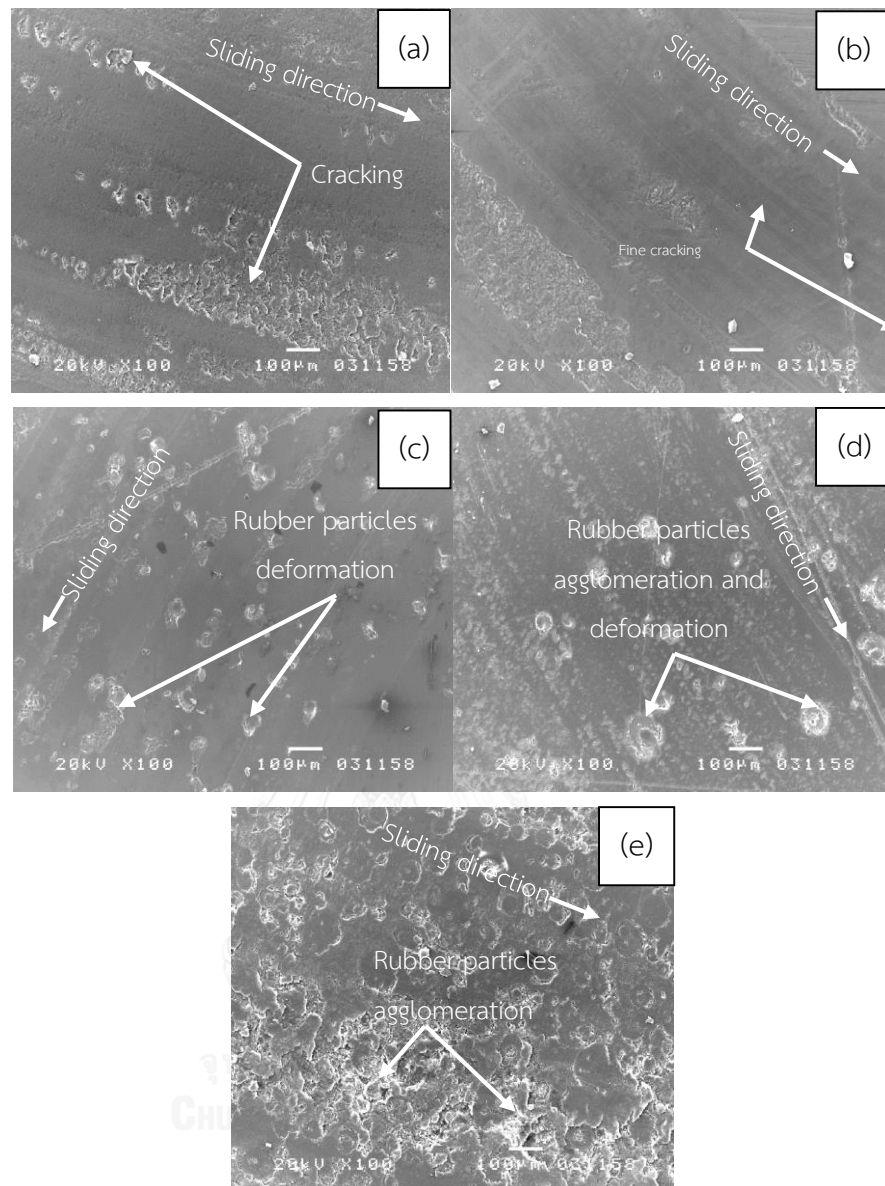
Figure 5.15 Worn surface of UNBR-filled polybenzoxazine composites: (a) neat
polybenzoxazine (PBA-a), PBA-a filled with (b) 2wt%, (c) 5wt%, (d) 10wt%
and (d) 15wt% of UNBR after friction test at 1000 m in distance at room
temperature.
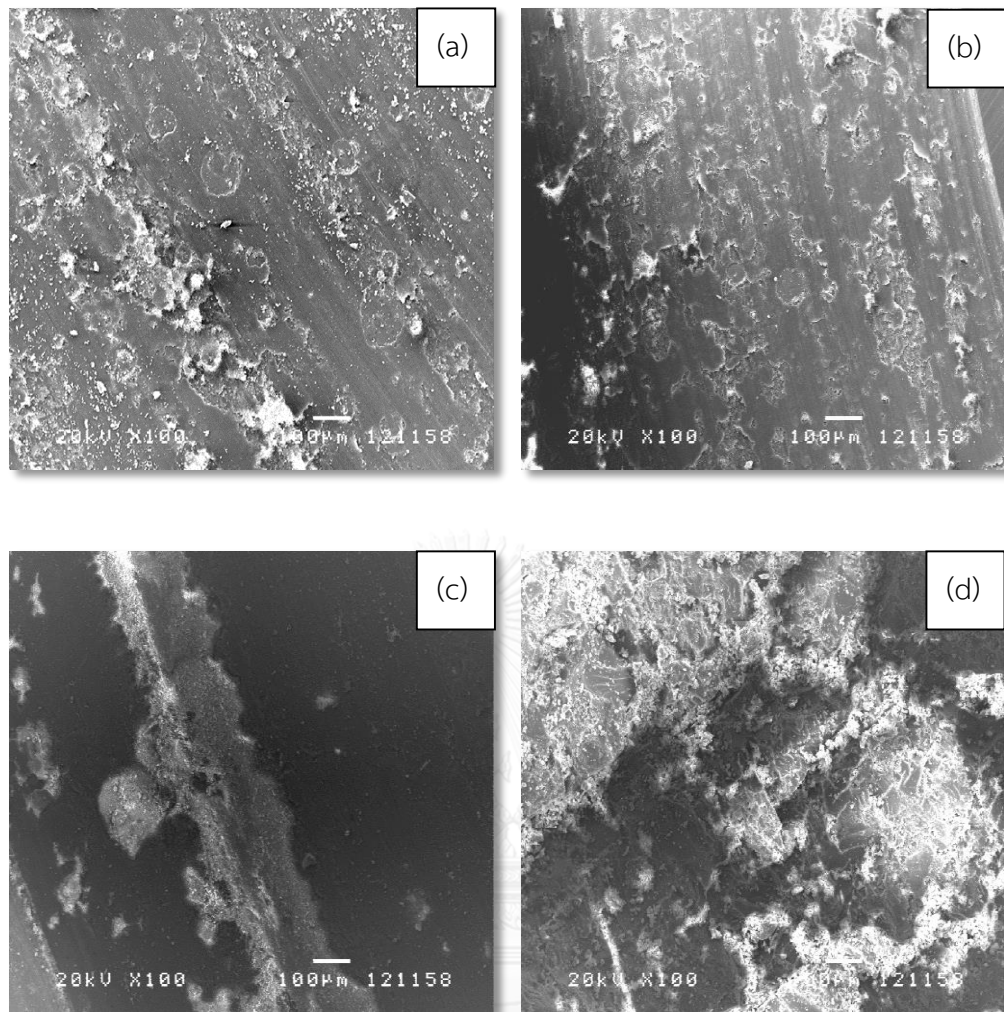
Figure 5.16 Worn surface of 5wt% of ultrafine-NBR (UNBR) filled polybenzoxazine
composite at various sample temperatures: (a) 100°C (b) 150°C, (c) 200°C
and (d) 250°C.

Table 5.3 Formulation of PBA-a based and phenolic based composites for brake pads application [8]

Ingredient	Phenolic based (wt%)	PBA-a based (wt%)
Benzoxazine resin	0	10
Phenolic resin	10	0
Aramid pulp	5	5
Copper fiber	10	10
Iron fiber	25	25
Zirconium silicate	7	7
Barium sulfate	25	25
Graphite	10	10
UNBR	4	4
Cashew dust	4	4

Table 5.4 Thermal, machanical, friction and wear properties of PBA-a based and phenolic based composites for brake pads application

Properties	Phenolic based composite	PBA-a based composite
T_g from tan delta ($^{\circ}$C)	210	215
T_{d5} ($^{\circ}$C)	424	410
Residual at 800°C (wt%)	80	79
COF at room temperature	0.29	0.35
Specific wear rate ($10^{-4} \times$mm^3 /Nm)	0.58	0.43
Storage modulus at 30°C (GPa)	2.9	6.2
Flexural strength (MPa)	33±2	61±4
Flexural modulus (GPa)	3.3±0.2	6.4±0.3

CHAPTER VI

CONCLUSIONS

The adhesion between the NBR particles and PBA-a was observed to be strong with relatively uniform distribution of the particulate fillers. The FTIR result suggested the formation of C-O-C bond between the polybenzoxazine and the NBR fillers. Storage modulus of the UNBR and MNBR composites was decreased with increasing content of rubber particles. The glass transition temperature measured from the peak of the loss modulus was substantially increased with the addition of the UNBR or MNBR particles in composite. These property enhancements were likely due to the strong interfacial bonding observed in the composites. Furthermore, degradation temperature of the PBA-a/UNBR and PBA-a/MNBR composites was found to decrease with the increase of rubber particles content. In term of tribological properties, the coefficient of friction (COF) of the PBA-a/MNBR and PBA-a/UNBR composite found to increase with increasing rubber particles content. The specific wear rate of the composites showed the minimal value at rubber particles content 5wt%. Furthermore, the PBA-a filled with 5wt% of UNBR can maintain the COF in the range of 0.51 to 0.60 at temperature range 100 to 250°C.

Finally, the results show that the benzoxazine resin modified with UNBR is suitable for applied in brake pads application.

REFERENCES

[1]   Industry, T.A.I.M.o., <u>Master Plan for Automotive Industry 2012 – 2016</u>. 2012. p. 1-2.

[2]   Day, A., <u>Chapter 10 - Brake Noise and Judder, in Braking of Road Vehicles</u>, A. Day, Editor. 2014, Butterworth-Heinemann: Oxford. p. 343-384.

[3]   Liew, K.W. and Nirmal, U., Frictional performance evaluation of newly designed brake pad materials. <u>Materials & Design</u>, 2013. 48(0): p. 25-33.

[4]   Thorpe, A. and Harrison, R.M., Sources and properties of non-exhaust particulate matter from road traffic: A review. <u>Science of The Total Environment</u>, 2008. 400(1–3): p. 270-282.

[5]   Bijwe, J., Composites as friction materials: Recent developments in non-asbestos fiber reinforced friction materials—a review. <u>Polymer Composites</u>, 1997. 18(3): p. 378-396.

[6]   Bijwea, J., Nidhi, Majumdarb, N., and Satapathy, B.K., Influence of modified phenolic resins on the fade and recovery behavior of friction materials. <u>Wear</u>, 2005. 259: p. 1068-1078.

[7]   Anthony, R., Mary, J., Kumar, V., and Teh-Kwang, P., *Resin mixture for friction materials* 1997.

[8]   Kurihara, S., Idei, H., Aoyagi, Y., and Kuroe., M., *Binder resin for friction material*, 2012.

[9]   Gurunath, P.V. and Bijwe, J., Potential exploration of novel green resins as binders for NAO friction composites in severe operating conditions. <u>Wear</u>, 2009. 267(5–8): p. 789-796.

[10]   Rimdusit, S., Tiptipakorn, S., Jubsilp, C., and Takeichi, T., Polybenzoxazine alloys and blends: Some unique properties and applications. <u>Reactive and Functional Polymers</u>, 2013. 73(2): p. 369-380.

[11]   Allen, D.J. and Ishida, H., Polymerization of linear aliphatic diamine-based benzoxazine resins under inert and oxidative environments. <u>Polymer</u>, 2007. 48(23): p. 6763-6772.

[12]   Chernykh, A., Agag, T., and Ishida, H., Novel benzoxazine monomer containing diacetylene linkage: An approach to benzoxazine thermosets with low polymerization temperature without added initiators or catalysts. Polymer, 2009. 50(14): p. 3153-3157.

[13]   Choi, S.-W., Ohba, S., Brunovska, Z., Hemvichian, K., and Ishida, H., Synthesis, characterization and thermal degradation of functional benzoxazine monomers and polymers containing phenylphosphine oxide. Polymer Degradation and Stability, 2006. 91(5): p. 1166-1178.

[14]   Ishida, H. and Sanders, D.P., Regioselectivity of the ring-opening polymerization of monofunctional alkyl-substituted aromatic amine-based benzoxazines. Polymer, 2001. 42(7): p. 3115-3125.

[15]   Brake pads and work mechanism [cited 2014 24]; Available from: http://4wheelonline.com/atv/ATV_Brake_Pads_and_Shoes.105333.

[16]   Eriksson, M., Bergman, F., and Jacobson, S., On the nature of tribological contact in automotive brakes. Wear, 2002. 252(1–2): p. 26-36.

[17]   Eriksson, M., Lord, J., and Jacobson, S., Wear and contact conditions of brake pads: dynamical in situ studies of pad on glass. Wear, 2001. 249(3): p. 272-278.

[18]   Nidhi and Bijwe, J., NBR-modified resin in fade and recovery module in non-asbestos organic (NAO) friction materials. Tribology Letters, 2007. 27(2): p. 189-196.

[19]   Liu, X., Wang, H., Wu, X., Bu, J., and Cong, P., Effect of the Rubber Components on the Mechanical Properties and Braking Performance of Organic Friction Materials. Journal of Macromolecular Science, Part B, 2013. 53(4): p. 707-720.

[20]   Kumar, M. and Bijwe, J., Non-asbestos organic (NAO) friction composites: Role of copper; its shape and amount. Wear, 2011. 270(3–4): p. 269-280.

[21]   Kumar, M. and Bijwe, J., Role of different metallic fillers in non-asbestos organic (NAO) friction composites for controlling sensitivity of coefficient of friction to load and speed. Tribology International, 2010. 43(5–6): p. 965-974.

[22]   Chan, D. and Stachowiak, G.W., Review of automotive brake friction materials. Journal of Automobile Engineering, Proceedings of the Institution of Mechanical Engineers Part D, 2004. 218(9): p. 953-966.

[23]   Jang, H. and Kim, S.J., The effects of antimony trisulfide (Sb_2S_3) and zirconium silicate ($ZrSiO_4$) in the automotive brake friction material on friction characteristics. Wear, 2000. 239(2): p. 229-236.

[24]   Friedrich, K. and Schlarb, A.K., *Tribology of Polymeric Nanocomposites:Friction and Wear of Bulk Materials and Coatings*, 2013, Butter-worth-Heinemann: UK. p. 23-37.

[25]   Gandra, J., Krohn, H., Miranda, R.M., Vilaça, P., Quintino, L., and dos Santos, J.F., Friction surfacing—A review. Journal of Materials Processing Technology, 2014. 214(5): p. 1062-1093.

[26]   Findik, F., Latest progress on tribological properties of industrial materials. Materials & Design, 2014. 57(0): p. 218-244.

[27]   Heisler, H., 11 - Brake system, in Advanced Vehicle Technology (Second Edition), H. Heisler, Editor. 2002, Butterworth-Heinemann: Oxford. p. 450-509.

[28]   Tribology and definition [cited 2014 24 February]; Available from: http://www.lehigh.edu/~intribos/tribology.html.

[29]   Wallbridge, N.C. and Dowson, D., Distribution of wear rate data and a statistical approach to sliding wear theory. Wear, 1987. 119(3): p. 295-312.

[30]   Jacobs, O. and Schädel, B., Chapter 9 - Wear behavior of carbon nanotube-reinforced polyethylene and epoxy composites, in Tribology of Polymeric Nanocomposites (Second Edition), K. Friedrich and A.K. Schlarb, Editors. 2013, Butterworth-Heinemann: Oxford. p. 307-352.

[31]   Karger-Kocsis, J., Mousa, A., Major, Z., and Békési, N., Dry friction and sliding wear of EPDM rubbers against steel as a function of carbon black content. Wear, 2008. 264(3–4): p. 359-367.

[32]   Wang, L.L., Zhang, L.Q., and Tian, M., Mechanical and tribological properties of acrylonitrile–butadiene rubber filled with graphite and carbon black. Materials & Design, 2012. 39(0): p. 450-457.

[33]   Meyer, K., A. Dorinson, K. C. Ludema. Mechanics and Chemistry in Lubrication. Tribology Series, 9. Elsevier; Amsterdam - Oxford -New York -Tokyo 1985, 634 Seiten. US $ 120.25, Dfl. 325.00, ISBN 0-444-42492-X. Crystal Research and Technology, 1986. 21(7): p. 858-858.

[34]   Johanson, C. and Stockel, M.T., Auto Brakes, ed. 3. 2008.

[35]   Kumar, M. and Bijwe, J., Studies on reduced scale tribometer to investigate the effects of metal additives on friction coefficient – Temperature sensitivity in brake materials. Wear, 2010. 269(11–12): p. 838-846.

[36]   Stadler, Z., Krnel, K., and Kosmac, T., Friction behavior of sintered metallic brake pads on a C/C–SiC composite brake disc. Journal of the European Ceramic Society, 2007. 27(2–3): p. 1411-1417.

[37]   McKenzie, E.R., Money, J.E., Green, P.G., and Young, T.M., Metals associated with stormwater-relevant brake and tire samples. Science of The Total Environment, 2009. 407(22): p. 5855-5860.

[38]   Mathissen, M., Scheer, V., Vogt, R., and Benter, T., Investigation on the potential generation of ultrafine particles from the tire–road interface. Atmospheric Environment, 2011. 45(34): p. 6172-6179.

[39]   Harifi, A., Aghagolzadeh, A., Alizadeh, G., and Sadeghi, M., Designing a sliding mode controller for slip control of antilock brake systems. Transportation Research Part C: Emerging Technologies, 2008. 16(6): p. 731-741.

[40]   Kanarek, M.S., Mesothelioma from Chrysotile Asbestos: Update. Annals of Epidemiology, 2011. 21(9): p. 688-697.

[41]   Ishida, H. and Allen, D.J., Mechanical characterization of copolymers based on benzoxazine and epoxy. Polymer, 1996. 37(20): p. 4487-4495.

[42]   Ning, X. and Ishida, H., Phenolic materials via ring-opening polymerization: Synthesis and characterization of bisphenol-A based benzoxazines and their polymers. Journal of Polymer Science Part A: Polymer Chemistry, 1994. 32(6): p. 1121-1129.

[43]   Baqar, M., Agag, T., Ishida, H., and Qutubuddin, S., Polymerization behavior of methylol-functional benzoxazine monomer. Reactive and Functional Polymers, 2013. 73(2): p. 360-368.

[44]   Ishida, H. and Agag, T., Handbook of Benzoxazine Resin. 2012: Oxford: Elsevier Press.

[45]   Nair, C.P.R., Advances in addition-cure phenolic resins. Progress in Polymer Science, 2004. 29(5): p. 401-498.

[46]   online, e.b. *nitrile rubber (NBR)*. 2014   [cited 2014 july 24]; Available from: http://www.britannica.com/EBchecked/topic/416122/nitrile-rubber.

[47]   Sreeja, R., Najidha, S., Remya Jayan, S., Predeep, P., Mazur, M., and Sharma, P.D., Electro-optic materials from co-polymeric elastomer–acrylonitrile butadiene rubber (NBR). <u>Polymer</u>, 2006. 47(2): p. 617-623.

[48]   Stiicklin, P. and Konrad, E., *Unvulcanized and vulcanized compositions*, 1934.

[49]   Ishida, H. and Allen, D.J., Physical and mechanical characterization of near-zero shrinkage polybenzoxazines. <u>Journal of Polymer Science Part B: Polymer Physics</u>, 1996. 34(6): p. 1019-1030.

[50]   Lu, Y., A combinatorial approach for automotive friction materials: Effects of ingredients on friction performance. <u>Composites Science and Technology</u>, 2006. 66(3–4): p. 591-598.

[51]   Nakamura, T., Nagata, T., Takeuchi, K., and Kobayashi, M., *Non-asbestos friction materials*, 2003.

[52]   Saffar, A. and Shojaei, A., Effect of rubber component on the performance of brake friction materials. <u>Wear</u>, 2012. 274–275(0): p. 286-297.

[53]   Jubsilp, C., Taewattana, R., Takeichi, T., and Rimdusit, S., Investigation on Rubber-Modified Polybenzoxazine Composites for Lubricating Material Applications. <u>Journal of Materials Engineering and Performance</u>, 2015. 24(10): p. 3958-3968.

[54]   Kupreev, A.V., Development and study of combined phenol-rubber binders for frictional composites. <u>Journal of Friction and Wear</u>, 2012. 33(6): p. 479-484.

[55]   Wu, Y., Zeng, M., Xu, Q., Hou, S., Jin, H., and Fan, L., Effects of glass-to-rubber transition of thermosetting resin matrix on the friction and wear properties of friction materials. <u>Tribology International</u>, 2012. 54(0): p. 51-57.

[56]   Kaynak, C. and Cagatay, O., Rubber toughening of phenolic resin by using nitrile rubber and amino silane. <u>Polymer Testing</u>, 2006. 25(3): p. 296-305.

[57]   Chonkaew, W., Sombatsompop, N., and Brostow, W., High impact strength and low wear of epoxy modified by a combination of liquid carboxyl terminated poly(butadiene-co-acrylonitrile) rubber and organoclay. <u>European Polymer Journal</u>, 2013. 49(6): p. 1461-1470.

APPENDIX

APPENDIX A

Characterization of UNBR and MNBR filled Polybenzoazine Composites

Appendix A-1 The actual density of MNBR filled polybenzoxazine and UNBR filled polybenzoxazine composites.

MNBR content (wt%)	UNBR content (wt%)	Theoretical density (g/cm^3)	Actual density of MNBR composites (g/cm^3)	Actual density of UNBR composites (g/cm^3)
0	0	1.1900	1.1900	1.1900
2	25	1.1864	1.1861	1.1864
5	5	1.1810	1.1810	1.1809
10	10	1.1720	1.1719	1.1720
15	15	1.1630	1.1628	1.1630

Appendix A-2 The storage modulus (E´) at 30°C and the glass transition temperature (T$_g$, loss modulus), of MNBR filled polybezoxazine composites at various graphite contents which were determined from DMA.

MNBR content (wt%)	Storage modulus (E´) at 30°C (GPa)	Glass transition temperature (^{o}C)
0	5.2	170
2	4.8	176
5	3.8	182
10	3.3	185
15	2.8	186

Appendix A-3 The storage modulus (E′) at 30°C and the glass transition temperature (T$_g$, loss modulus), of UNBR filled polybezoxazine composites at various graphite contents which were determined from DMA.

UNBR content (wt%)	Storage modulus (E′) at 30°C (GPa)	Glass transition temperature (°C)
0	5.2	170
2	4.7	175
5	3.7	182
10	3.3	185
15	2.7	188

VITA

Mr. Jakkrit Jantaramaha was born in Surat Thani, Thailand. He graduated at high school level in 2009 from Suratpittaya School. He received the Bachelor's Degree of Engineer with a major in Chemical Engineering from the Faculty of Engineer, Srinakharinwirot University, Thailand in 2013. After graduation, he entered study for a Master's Degree of Chemical Engineering at the Department of Chemical Engineering, Faculty of Engineering, Chulalongkorn University.

Some part of this work was selected for oral presentation in The 8th International Conference on Materials Science and Technology or MSAT-8 which was held during December 15-16, 2014 at Swissotel Le Concerde, Bangkok, Thailand.